AGARD-AR-184

AGARD-AR-184

AGARD

ADVISORY GROUP FOR AEROSPACE RESEARCH & DEVELOPMENT

7 RUE ANCELLE 92200 NEUILLY SUR SEINE FRANCE

AGARD ADVISORY REPORT No. 184

Wind Tunnel Flow Quality and Data Accuracy Requirements

NORTH ATLANTIC TREATY ORGANIZATION

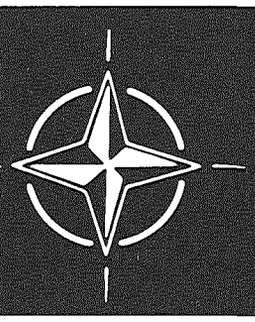

AGARD ADVISORY REPORT No. 184

"Wind Tunnel Flow Quality and Data Accuracy Requirements"

ERRATA

Page 1 - Second paragraph, first line:
Amend to read
It was found in more than a few situations, that the ....

Page 3 - Last paragraph but one (Side-wall effects), second line:
Amend to read
(e.g., Refs. 3, 4, and 4a)

Page 5 - Second paragraph, first line:
Amend to read
Wall corrections: The effects .... depend on the model and wall geometry ...

- Paragraph 2.3 (Boundary-Layer Measurements), second line:
Amend to read
... should be obtained are not quoted.

Page 7 - Second paragraph, third line:
Amend to read
.... specifications, typical acceptable bias and deviation ....

Page 18 - First paragraph, line six:
Amend to read
.... to the measurement of angle of attack ....

Page 19 - REFERENCES
After reference 4, add
4a. Chan Y.Y.: Boundary Layer Control on the Side-walls on Windtunnels for Two-Dimensional Tests. J. Aircraft, Vol. 17, May 1980

NORTH ATLANTIC TREATY ORGANIZATION

ADVISORY GROUP FOR AEROSPACE RESEARCH AND DEVELOPMENT

(ORGANISATION DU TRAITE DE L'ATLANTIQUE NORD)

AGARD Advisory Report No.184

WIND TUNNEL FLOW QUALITY AND DATA ACCURACY REQUIREMENTS

by

F.Steinle
NASA AMES Research Center
Moffett Field
CA 94035 – USA

and

E.Stanewsky
DFVLR-AVA
Bunsenstrasse 10
3400 Göttingen – FRG

Edited by

R.O.Dietz
Route 1
Manchester, Tennessee 37355 – USA

sponsored by

The Windtunnel Testing Techniques Sub-Committee
of the
Fluid Dynamics Panel

This Advisory Report was prepared for the Fluid Dynamics Panel of AGARD.

THE MISSION OF AGARD

The mission of AGARD is to bring together the leading personalities of the NATO nations in the fields of science and technology relating to aerospace for the following purposes:

- Exchanging of scientific and technical information;
- Continuously stimulating advances in the aerospace sciences relevant to strengthening the common defence posture;
- Improving the co-operation among member nations in aerospace research and development;
- Providing scientific and technical advice and assistance to the North Atlantic Military Committee in the field of aerospace research and development;
- Rendering scientific and technical assistance, as requested, to other NATO bodies and to member nations in connection with research and development problems in the aerospace field;
- Providing assistance to member nations for the purpose of increasing their scientific and technical potential;
- Recommending effective ways for the member nations to use their research and development capabilities for the common benefit of the NATO community.

The highest authority within AGARD is the National Delegates Board consisting of officially appointed senior representatives from each member nation. The mission of AGARD is carried out through the Panels which are composed of experts appointed by the National Delegates, the Consultant and Exchange Programme and the Aerospace Applications Studies Programme. The results of AGARD work are reported to the member nations and the NATO Authorities through the AGARD series of publications of which this is one.

Participation in AGARD activities is by invitation only and is normally limited to citizens of the NATO nations.

Published November 1982

ISBN 92-835-1440-8

Printed by Technical Editing and Reproduction Ltd
5–11 Mortimer Street, London, W1N 7RH

CONTENTS

	Page
SUMMARY	1
SYMBOLS	1
1. INTRODUCTION	2
1.1. Scope and Definition of Work	2
2. COMPILATION OF DATA ACCURACY AND FLOW-QUALITY REQUIREMENTS	3
2.1 Steady-State and Dynamic Pressure Measurements	3
2.2 Force and Moment Measurements (Balance Measurements)	4
2.3 Boundary-Layer Measurements	5
2.4 Unsteady Phenomena	6
2.5 Simulated Engine Flow	6
2.6 Reflection-Plane Testing	6
3. DETAILED EXAMINATION OF THE EFFECT OF FLOW QUALITY ON DATA ACCURACY: FORCES AND MOMENTS	6
3.1 Formulation of the Basic Model	7
3.2 Discussion of Contributions	8
3.3 Summary of Deviation Effects	15
4. OTHER TYPES OF MEASUREMENTS	15
4.1 Laminar Flow Control Technology	15
4.2 Determination of Boundary-Layer Properties by Holographic Methods	15
4.3 Desirable Particulate in the Flow Field for Laser Velocimetry	16
4.4 Tunnel Cleanliness	17
5. SUMMARY OF FLOW-QUALITY AND DATA-ACCURACY REQUIREMENTS	17
5.1 Flow Quality	17
5.2 Data Accuracy	17
6. CONCLUDING REMARKS	18
7. RECOMMENDATIONS	18
APPENDIX – CONVENERS GROUP	18
REFERENCES	19
TABLE	21
FIGURES	22

WIND TUNNEL FLOW QUALITY AND DATA ACCURACY REQUIREMENTS

Report of the AGARD FDP TES Conveners Group

SUMMARY

This report is written by the Wind Tunnel Testing Techniques (TES)* Subcommittee of the AGARD Fluid Dynamics Panel. It deals with flow quality and data accuracy requirements for wind tunnel testing. The emphasis is on transonic test conditions. Two conveners, one from each side of the Atlantic, were appointed by the TES Subcommittee. The conveners brought together the foremost workers for purposes of discussing the current level of testing technology, what are the requirements of the future, and what needs to be done.

It was found in more than a few situations, the requirements for data accuracy and flow quality are not well defined. The requirements that are compiled represent the current thinking. To aid in understanding the impact of flow quality and data accuracy, included in this study is a detailed examination of their contributions to the test results of a transport-type configuration. The approach can be adapted to other types. The results of this effort correlate well with what is generally accepted.

The result of this effort brought focus on the need to document the flow quality in each facility and that the measurements should include a standard set of both instrumentation and data reduction methods. Aside from the already well-known need to improve angle-of-attack measuring capability, the need to understand the role of aero-noise on Reynolds number effects was highlighted.

SYMBOLS

A	amplitude
A	aspect ratio
A_{bc}	base or cavity area
A_n	normal area
C	number density
C_c	chord or axial-force coefficient, $F_C/q_\infty S$
C_D	drag coefficient, drag/$q_\infty S$
C_f	coefficient of skin friction
C_L	lift coefficient, lift/$q_\infty S$
C_ℓ	section lift coefficient
C_M	pitching moment coefficient, moment/$q_\infty S\bar{c}$
C_N	normal-force coefficient, $F_N/q_\infty S$
c	chord
$\bar{c}$	mean aerodynamic chord
c_p	pressure coefficient, $(p - p_\infty)/q_\infty$
c_p'	dimensionless rms pressure fluctuation
d_p	particle diameter
e	span efficiency factor
e	exit conditions
e	elliptical
F	force
F_C	chord force
F_N	normal force
f	skin friction
g	acceleration due to gravity
g	gas
i	inlet
i	incidence angle
k	surface roughness
L	fuselage length
L	optical path length
ℓ	mean free path
ℓ_t	tail length in tail volume coefficient
ℓ_x	integral spatial correlation
M	free-stream Mach number
n	reduced frequency
$[nF(n)]^{1/2}$	$c_p'(\Delta n/n)^{-1/2}$ in bandwidth Δn at reduced frequency n
$\dot{n}$	data rate
o	root
P	static pressure
P_t	total pressure
$\langle p' \rangle$	rms value of fluctuating pressure
p	particle
p	parabolic
p'	fluctuating component of static pressure
q	dynamic pressure
Re	Reynolds number
rms	root mean square
S	reference area
S_w	wetted area
S_{we}	effective wetted area
T	end of transition

*TES — Techniques d'Essais en Souffleries (French equivalent of Wind Tunnel Testing Techniques).

T	temperature	ν	kinematic viscosity
T_o	stagnation temperature	ξ	dummy variable
t	transonic	ρ	density
U	streamwise velocity	ρ'	fluctuations in density
u'	fluctuating component of velocity	σ	standard deviation
u_τ	shear-stress velocity, $(\tau_w/\rho)^{1/2}$	τ_w	wall shear stress
V	model volume	< >	root mean square
W	weight flow	Subscripts	
w	upflow velocity component	b	base
X	streamwise coordinate	bc	base or cavity
Y	ordinate of camber line	c	cavity
α	angle of attack	des	design
α_1	scaling parameter, induced camber	F	force
Δ	change	fs	full-scale
δ	scaling parameter, parabolic lift	i	dummy index
ε	precision/accuracy of proportionality	int	internal
θ	duct exit flow angle	t	stagnation
κ	Cunningham constant = 1.8 for air	t	tail
λ	wavelength	∞	free stream
μ	coefficient of viscosity	γ	ratio of specific heats at constant pressure and volume, 1.4 for air

1. INTRODUCTION

1.1 Scope and Definition of Work

A recent effort to establish an experimental data base for computer program assessment has shown that there is a scarcity of reliable information on flow quality and data accuracy in existing subsonic and transonic wind tunnels (Ref. 1) needed to establish higher confidence in the data base. Furthermore, it was realized that the effect of flow quality on data accuracy was not in all instances well understood and that there was only limited information on the data accuracy — and hence on the flow quality — actually required for a specific test. In recognition of these problems, of the necessity for future improvements of existing wind tunnels, and of the need to provide guidance for the designer of new facilities, a Conveners Group was formed by the AGARD FDP (members are listed in the Appendix) with the objective of specifying, for subsonic and transonic speeds, data-accuracy and flow-quality requirements in relation to the following:

1. Steady-state and dynamic-pressure measurements
2. Force and moment measurements
3. Boundary-layer and heat-transfer measurements
4. Component force measurements
5. Buffeting, flutter, and dynamic stability investigations

Consideration was also to be given to specific types of testing:

1. Experiments with simulated engine flow
2. Reflection-plane testing

The Conveners Group was to specify for a given accuracy and for the types of testing listed above the following:

1. Distribution and fluctuations throughout the test section of total and static pressure; velocity, including direction and magnitude; and temperature
2. Frequency spectra of disturbances such as flow turbulence, and acoustic effects due to tunnel drive system, wall vibrations, reflection waves, and wall boundary layer
3. Purity of fluid

4. Wind-tunnel and support-interference corrections for steady, oscillatory, and rotary experiments with full and half models

5. Model surface tolerance and aeroelastic design requirements

6. Measurements of and corrections for aeroelastic deformations and vibrations of models and support systems

The accuracy requirements for wind-tunnel data were to be specified in relation to

1. The prediction of performance and operating characteristics of a given configuration

2. The evaluation of differences in performance due to small configurational changes

3. The assessment of computational codes

1.2 Complexity of Task and Approach

In the overall sense, the goal of the airframe manufacturer, insofar as the use of wind-tunnel data is concerned, is to be able to incorporate those data into the most reliable prediction of flight performance that can be made within the constraint of cost effectiveness. In this sense, uncertainties in the data are directly transferable to uncertainties in predicted performance. As indicated above, many kinds of tests comprise the data base used to predict performance; both absolute and incremental quantities — the latter in the refinement process of the design — are of importance. In research, the goal regarding wind-tunnel data is to use the data with confidence, without having inaccuracies or imprecision obscure or preclude achieving the research objectives.

All the data are affected by the test technique used, the flow quality of the tunnel, and the uncertainty of the measurements. All foregoing items interact. The complexity of this interaction between the flow environment produced by the facility and the measurement itself results in the overall data uncertainty; this interaction is illustrated in Fig. 1 (Ref. 2).

As one can see, the goals set forth by the initiators of the Group are formidable. The large number of parameters involved and the limited time given the Group — at least initially — made it impossible to cover all types of measurements and influence-parameters in a satisfactory way. In view of this, the Group took the following approach:

1. Compile, to the extent possible, quantitative and qualitative information on data accuracy and establish the corresponding flow-quality requirements for the types of measurements specified above. These results, corresponding to the scope and definitions of work outlined, are contained in Table 1. Where necessary, discussion of results is in Sec. 2 of this report.

2. Examine in detail the effects of flow quality on static stability and control-type testing with emphasis on the most crucial aerodynamic parameter, that is, drag.

2. COMPILATION OF DATA-ACCURACY AND FLOW-QUALITY REQUIREMENTS

The following qualitative and quantitative assessment of data-accuracy and flow-quality requirements is very preliminary in nature; it is not to be construed as a detailed investigation of the subject. One should, therefore, keep in mind that future discussions may to some extent alter the information presented here. The presentation in this section follows in general the order shown in Table 1. This table contains, besides numbers quoted on accuracy and flow quality, an indication of which influence-parameters are less important for a particular type of measurement and where the more relevant parameters are discussed.

2.1 Steady-State and Dynamic Pressure Measurements

The data accuracies quoted for steady-state pressure measurements on model surfaces are as follows:

1. Performance verification : $\Delta c_p = 0.01$

2. Small configurational changes : $\Delta c_p = 0.001$

3. Assessing computer codes : $\Delta c_p = 0.01$

The accuracy requirement for (2) is derived from the desired accuracy in pressure drag prediction of $\Delta C_{Dp} \approx 0.0001$. The flow-quality requirements are generally the same as the ones for force measurements. Overlapping requirements will, therefore, be discussed in the respective section.

The data accuracy requirements for dynamic pressure measurements are similar to the ones for steady-state pressure measurements.

Side-wall effects — Side-wall effects with two-dimensional models have been considered by various investigators (e.g., Refs. 3,4); however, the results are still not conclusive. Within the activities of the GARTEur Action Group on Two-Dimensional Testing Methods, these effects will be further investigated.

Aeroelastic effects — Model vibrations at the model and sting natural frequencies are easy to measure by equipping the model with accelerometers (a minimum of six is required). However, correcting pressures in dynamic tests can only be done for motions in the first wing-bending or rigid-body modes. Consequently, stiffer models — for instance, those made of carbon fibre — should be used in the interest of obtaining accurate pressure data.

2.2 Force and Moment Measurements (Balance Measurements)

The information given here is based on requirements for transport-type aircraft in the high-speed regime, with drag being considered the most important aerodynamic parameter to be determined.

Repeatability and minor configuration changes — The accuracy requirements for lift, drag, and pitching moment, as stated by various research and industry sources, are:

Lift coefficient	$\Delta C_L = 0.01$
Drag coefficient	$\Delta C_D = 0.0001$
Pitching-moment coefficient	$\Delta C_M = 0.001$

To achieve the required drag accuracy within the range of the rapid drag variation at the drag divergence boundary, the free-stream Mach number must be determined and kept constant for the period of at least one α-sweep to within $\Delta M = 0.001$. Generally, the flow uniformities are not important as long as they stay the same over prolonged periods of time. In this respect, one must be careful with tunnel modifications and unwanted changes to the tunnel circuit — for example, an accumulation of dirt in coolers and screens may alter local conditions in the test section.

To maintain the required accuracies over the number of runs necessary to evaluate the effect of configurational changes — large or small — one must be able to repeat the free-stream conditions within certain boundaries. These boundaries are as follows:

1. Tunnel total and stagnation pressure: 0.1%
2. Model angle of attack: 0.01°
3. Mach number (as above): 0.001

Furthermore, one must be careful that the model geometry and the surface finish do not change during the time a test series is conducted or when certain test conditions are repeated (model aging).

Assessment of major configurational changes and model comparisons — The accuracy requirements for lift, drag, and pitching moment are the same as stated in the preceding subsection; however, the flow-quality requirements are more stringent, depending on the model changes, for example, changes in wing area and span, body length and cross-sectional area, and position of tail surface.

Flow nonuniformities: The requirement for the pressure variation along the model axis is given by the desired drag accuracy. Assuming a ratio of 0.1 between body cross-sectional and wing area, it follows for

$$\Delta C_D = 0.0001 \rightarrow \Delta c_p = 0.001$$

over the length of the model. The required accuracy in drag also determines the accuracy of the flow angle at the wing location. The latter follows from the relation $C_D \cong C_N \cdot \alpha + C_c$, where C_N and C_c are the normal- and axial-force coefficients, respectively, measured by the balance. Assuming a normal-force coefficient of $C_N \cong 0.5$ at cruise, one obtains for

$$\Delta C_D = 0.0001 \rightarrow \Delta\alpha = 0.01°$$

This also sets the required accuracies for C_N and C_c.

The required accuracy in flow angularity at the tail location — and hence in the axial variation in flow angularity — is derived from the accuracy requirement for the pitching moment. Assuming a tail volume of 0.1 and a $(dC_L/d\alpha)_{tail}$ of 0.1/deg, it follows from

$$\Delta C_M = 0.001 \rightarrow \Delta\alpha = 0.1°$$

Total pressure and temperature variations over the span and the length of the model should be kept within 1/2% and ±1° K, respectively.

To obtain the required data accuracies, one should try to achieve a flow quality somewhat better than that indicated by the values given above. The flow-quality requirements may be met by design and calibration.

Flow unsteadiness: This is not a very critical parameter, unless very short measuring times are required. Evidence exists that significantly large flow unsteadiness can be induced by the model (e.g., by oscillating shock waves), to the extent that the unsteadiness levels of present day wind tunnels are exceeded. For the type of measurements considered here, adequate filtering techniques can be employed; however, sufficient run time must be provided (e.g., for static force and moment tests: 0.5 sec; for static pressure tests: 1 sec (Ref. 5)).

Flow unsteadiness will, of course, be important when tests are conducted in which there is free transition or in which there are boundary-layer measurements in general, or when specific tests, such as laminar flow control measurements, are conducted. These tests will actually set the flow-quality requirements here. They will be discussed further in Secs. 2.3 and 4.1.

Purity of fluid: Essentially two factors are of concern here: condensation effects and the impact of dust particles on the model surface. Condensation can be avoided by keeping the dew point 2° C below the free-stream static temperature (see Humidity in Sec. 3.2). Dust particles may increase the surface roughness

thus causing premature transition. Here, periodic checks and refinishing of the surface are necessary (see Sec. 4.4).

Wall corrections: The effects of tunnel-wall constraints on free-stream and local flow conditions depend on the model geometry and the flow field generated by that geometry. Hence, correction methods should be able to assess (1) relative changes in the free-stream flow conditions and (2) changes in local flow conditions at the wing location and along the model axis caused by configurational changes. Moreover, the correction methods should be able to assess these changes to accuracies of

$$\Delta\alpha = 0.01° \qquad \Delta M = 0.001$$

The range of lift and free-stream Mach numbers where these relative changes in flow conditions are of particular interest are $0.3 \leq C_L \leq 0.6$ and $0.5 \leq M \leq 0.85$.

Model support interference: Flow nonuniformities introduced by the model support should be known to the following accuracies:

At the tail location: $\Delta c_p < 0.001$ $\Delta\alpha < 0.1°$

At the wing location: $\Delta\alpha < 0.01$

A severe problem is the interference at the location where the sting enters the fuselage, because at that point base pressure, internal pressures, flow separation onset, and separation pattern may be affected. In general, the magnitude of the support interference may be checked and corrected for by using different support systems — for example, twin stings supporting the model from the wing tips while the forces on the afterbody are measured with and without the main sting present.

Model design tolerances: Here, only two statements were obtained:

1. Lifting surfaces should be manufactured to the following accuracies: ordinates, $\pm 0.0003\ \bar{c}$ ($\bar{c}$ = mean aerodynamic chord); and slope of ordinates, ±0.02°.

2. Local discontinuities in profile shape are more important than the absolute accuracy of the model. Discontinuities should not exceed 0.1°.

For surface finish requirements, see Sec. 2.3, Boundary-Layer Measurements.

Aeroelastic effects: Considering configurational changes, model deformation (wing twist) is not critical for $C_L - C_D$ comparisons but will influence $C_L - C_M$ comparisons. Because of the latter, wing-twist changes along the span should be known within $\Delta\alpha = 0.1°$. The wing deformation may be determined by static calibrations. For comments on model and sting vibrations see Secs. 2.1 and 2.4.

Absolute accuracy levels — The requirements for absolute accuracy when the aim is performance verification can be relaxed relative to those stated in the preceding sections, especially when considering drag. Here, an accuracy of $\Delta C_D = 0.0005$ (this is about the accuracy one is able to achieve in flight) is considered adequate. The corresponding accuracy in flow direction is about $\Delta\alpha = 0.05°$. Nevertheless, a higher accuracy is desirable since the final accuracy is a sum of many uncertainties. Of these, the translation from the wind-tunnel model to the real airplane, scale effects, and engine representation are probably the most important.

The data-accuracy requirements concerning computational fluid dynamics are equivalent to those for $\Delta C_D = 0.0001$.

2.3 Boundary-Layer Measurements

The accuracy requirements are similar to the ones for pressure measurements. Exact figures regarding the accuracy with which mean and fluctuating quantities and heat-transfer data should be obtained were not quoted. The figures on flow quality are summarized in Table 1.

Flow nonuniformities — The reason for the required flow quality is in part the extreme sensitivity of the boundary-layer development to convergence or divergence of edge streamlines (in plan view), the most common causes for this behavior being disturbances from screens, honeycomb, or corner vanes. Considering screens, the reader should be reminded that unmeasurably small free-stream disturbances (axial vorticity?) can produce spanwise variations of several percent in boundary-layer thickness or skin friction.

Flow unsteadiness — Experiments by Benek (Ref. 6) and Weeks and Hodges (Ref. 7) have shown a remarkable insensitivity of the boundary-layer development to sound waves, justifying the relatively high value of 2% q for pressure disturbances. A note of caution in this regard: when testing models with natural transition, the noise will promote earlier transition and hence there may be some significant displacement thickness effects as a result. Furthermore, there may be a small but significant effect of noise on skin friction for thin layers (see Reynolds number in Sec. 3.2). Considering vorticity, isotropic turbulence with a 0.1% rms u-component fluctuation causes somewhat more than 0.1% increase in flat-plate skin friction. Although lateral fluctuations in good tunnels exceed longitudinal fluctuations, 0.1% in the rms-value of the u-component is still considered conservative and even adequate for basic experiments on transition. (One exception, possibly, is LFC investigations, in which lower rms values are required; see Sec. 4.1.) At such low turbulent intensities, it is also sensible to assume that the turbulence structure has only minor effects on the boundary-layer development (Ref. 8).

The 0.5° K requirement for temperature spottiness is given here because temperature variations convected through a transonic or supersonic contraction lead to velocity fluctuations.

Purity of fluid — Purity of fluid is an important aspect in hot-wire measurements. Particles of the order of 1 μm may adhere to the wire, thus causing calibration changes, and particles of 10 μm or more may break the wire (see Secs. 4.3 and 4.4).

Support interference — At transonic speeds upstream influence of the probe and the probe support may appreciably distort the boundary layer. Quantitative rules are not available.

Model design — The requirements for model design are similar to the ones for force and moment measurements. In addition, a surface finish of $u_\tau k/\nu < 5$ is suggested.

2.4 Unsteady Phenomena

The flow-quality requirements for buffeting, flutter, and dynamic stability (quasi-steady derivatives) tests are given in Table 1. Remarks concerning the various influence-parameters are given below.

Flow nonuniformity — The low value of Mach number accuracy ($\Delta M = 0.01$) seems justified by the difficulty of modeling "unsteady phenomena." For buffeting or dynamic stability tests, one often encounters, for instance, separated flows with large scale effects. Again, if a model flutters at an equivalent air speed (EAS) of interest, it does not really matter if the Mach number is 0.97 or 0.98; however, the mode shapes and frequency parameters should be nearly correct.

For flutter tests, the temperature requirement is introduced, because the model stiffness varies with temperature, thus changing the desired stiffness distribution.

Flow unsteadiness — It is suspected that the flow-quality criteria given in AGARD Report No. 644, concerned with the high-Reynolds-number facility LEHRT (Ref. 9), are both unrealistic and unobtainable. There is good evidence that the NLR high-speed transonic tunnel is well suited for dynamic experiments. Here, the level of $\langle p'/q \rangle$ is about 0.5% and the parameter $[nF(n)]^{1/2}$ is about 0.002. These levels are close to the ones originally suggested by Mabey (Ref. 10). However, in any given facility it is important that support interferences, such as model support data and air supply struts, should not produce additional flow unsteadiness close to the model.

Model design — Surface finish of the model should correspond to the standards suggested by Bradshaw for boundary-layer measurements, i.e., $u_\tau k/\nu < 5$. It is, however, difficult to meet these standards for flutter models. The design for dynamic stability models should ensure tests at high angles of incidence since modern combat aircraft fly at high angles of attack (e.g., 0° to 90° in the low-speed range, 0° to 40° in the high-speed range).

Aeroelastic effects — In buffeting and dynamic stability tests model deformations should be measured. This might be accomplished by laser systems, which are presently being considered at RAE. Deformations of conventional flutter models are normally small, because they are tested at or near zero lift. For supercritical wings this is no longer true.

In dynamic stability tests the frequency parameters of interest are low; in buffeting investigations they are higher, but they can be separated from the frequencies of sting and model vibrations. The latter are, therefore, not important. In flutter tests the frequency parameter and mode shape of the vibration is important, but qualitative information is only required for the amplitudes.

2.5 Simulated Engine Flow

The flow-quality requirements for simulated engine flow are listed in Table 1.

Flow nonuniformity — The flow-quality requirements relative to flow nonuniformity derive from the necessity to accurately determine the intake buzz boundaries and the general pressure recovery.

Flow unsteadiness — The requirements that $\langle p_t' \rangle / p_t \leq 0.01$ ($\langle p_t' \rangle$ = rms of fluctuating total pressure) are a result of the sensitivity of modern compressors to badly designed intakes. If the flow unsteadiness is higher than the limit indicated, a bad design might not be identified from wind-tunnel tests.

Support interference — The support must be designed so that the entry flow is not altered.

Aeroelastic effects — The aeroelastic effects are normally small on the model but can be significant at full scale.

2.6 Reflection-Plane Testing

Reflection-plane testing should only be carried out to investigate configuration changes and to provide (wing) data for assessing computer codes. In that regard, the accuracy and flow-quality requirements are essentially similar to the ones for pressure and balance measurements. Investigations to assess the merit of reflection-plane testing are under way, for instance, at NLR, FFA, and DFVLR; however, it is still too early to draw any definite conclusions.

3. DETAILED EXAMINATION OF THE EFFECT OF FLOW QUALITY ON DATA ACCURACY: FORCES AND MOMENTS

The approach taken in examining the effects that flow quality has on data uncertainty is to concentrate on static stability and control-type testing with secondary emphasis on other types of measurements, including nonintrusive data methods.

Data uncertainty is composed of random error (scatter, noise, imprecision, etc.) and fixed error (bias, systematic error, etc.). The components of the random error, σ, contribute to the random error in the

root-square sense. Likewise, the components of the bias error, B_M, contribute to the total bias error. These two overall errors are then summed to produce the overall measurement undertainty, U_M, $U_M = \pm(B_M \pm 2\sigma)$.

Standard deviation is far easier to determine than bias error. In general, data that have small standard deviations lend confidence that the bias error is correspondingly small. Based on calibrations performed at the Ames Research Center and on comparisons with manufacturer's specifications, typical bias and deviation values are found to be as follows:

	B_M	2σ
Conventional strain gage pressure transducers	±0.15% FS	±0.12% FS
Semiconductor pressure transducers with second-order curve fit	±0.05% FS	±0.02→0.05% FS
Strain gage balance (controlled temperature)	±0.1% FS	±0.15% FS
Platinum resistance temperature transducer	±0.1% FS	±0.04% FS

For the purpose of estimating the overall uncertainty, the state of the art in transducers seems to be represented by bias errors roughly equivalent to the 2σ deviation. Therefore, the overall uncertainty of a measurement, to a first approximation, is

$$U_M = \pm(B_M \pm 2\sigma) = \pm(2\sigma \pm 2\sigma) = \pm 4\sigma$$

On this basis then, the following analysis which is centered on standard deviation is extendable to overall uncertainty.

Because the tunnel is not a steady flow environment, sufficient samples of data to establish the desired confidence level must be taken over a time interval sufficient to average out the effects of dynamic response and unsteady flow (Ref. 5). It is assumed that the data are acquired in this manner.

It is expected that this analysis, which is oriented to the drag of a transport-type configuration, will serve as a guide and that the reader will modify the results where required to fit a particular situation. Emphasis is on drag because of the impact this quantity has on performance (e.g., range, payload, transonic acceleration).

The general expression of the standard deviation in drag coefficient, σ_{C_D}, is

$$\sigma_{C_D} = \left[\sum_i \left(\frac{\partial C_D}{\partial \xi_i}\right)^2 \sigma_{\xi_i}^2\right]^{1/2}$$

3.1 Formulation of the Basic Model

The same general approach is followed as that taken in Ref. 11, in which Mach number, normal force, chord force, angle of attack, reference conditions, grit drag, internal flow, and wall interference in an error propagation analysis are treated. One can always set up an impossibly high goal, such as that the absolute drag uncertainty $\Delta C_D/C_D$ be within ±0.3%. In this event, subtle quantities have significant impact. A discussion and analysis of some of these factors are given in Ref. 11.

The general form is then:

$$\sigma_{C_D} = \left\{ \underbrace{\left[\frac{\partial C_D}{\partial M}\sigma_M\right]^2}_{\text{Mach number}} + \underbrace{\left[\frac{\partial C_D}{\partial F_N}\sigma_{F_N}\right]^2}_{\text{Normal force}} + \underbrace{\left[\frac{\partial C_D}{\partial F_C}\sigma_{F_C}\right]^2}_{\text{Chord force}} + \underbrace{\left[\frac{\partial C_D}{\partial \alpha}\sigma_\alpha\right]^2}_{\text{Angle of attack}} \right.$$

$$+ \underbrace{\left[\frac{\partial C_D}{\partial Re}\sigma_{Re}\right]^2}_{\text{Reynolds number}} + \underbrace{\left[\frac{\partial C_D}{\partial \frac{dM}{dX}}\sigma_{\frac{dM}{dX}}\right]^2}_{\text{Mach gradient}} + \underbrace{\left[\frac{\partial C_D}{\partial \frac{dW}{u_\infty\, dX}}\sigma_{\frac{dW}{u_\infty\, dX}}\right]^2}_{\text{Stream curvature}}$$

$$\left. + \underbrace{\left[\frac{\partial C_D}{\partial \frac{W}{u_\infty}}\sigma_{\frac{W}{u_\infty}}\right]}_{\text{Stream upwash}} + \underbrace{\left[\frac{\partial C_D}{\partial P_{bc}}\sigma_{P_{bc}}\right]}_{\text{Base or cavity pressure}} + \underbrace{\left[\sigma_{C_{D_{int}}}\right]^2}_{\text{Internal drag}} \right\}^{1/2}$$

In this form, the results are treated as being uncorrelated. Depending on how certain reference flow quantities are determined (Mach number, stagnation pressure, static pressure) and how the data are used, some elements should be recombined. For example, Re can be made up of contributions due to P_{t_∞}, M, T_t or $P_{t_\infty}, P_\infty, T_t$. Then with M made up of P_{t_∞} and P_∞ effects,

$$\left[\frac{\partial C_D}{\partial M}\sigma_M\right]^2 + \left[\frac{\partial C_D}{\partial Re}\sigma_{Re}\right]^2$$

should be rewritten as

$$\left[\frac{\partial C_D}{\partial M}\frac{\partial M}{\partial P_{t_\infty}} + \frac{\partial C_D}{\partial Re}\frac{\partial Re}{\partial P_{t_\infty}}\right]^2 \sigma^2_{P_{t_\infty}} + \left[\frac{\partial C_D}{\partial M}\frac{\partial M}{\partial P_\infty} + \frac{\partial C_D}{\partial Re}\frac{\partial Re}{\partial P_\infty}\right]^2 \sigma^2_{P_\infty} + \left[\frac{\partial C_D}{\partial Re}\frac{\partial Re}{\partial T_{t_\infty}}\right]^2 \sigma^2_{T_{t_\infty}}$$

Additionally, if the wind-tunnel data were to be adjusted to flight Reynolds number conditions, for example, then the term

$$\left[\frac{\partial C_D}{\partial Re}\sigma_{Re}\right]^2$$

should be treated as uncorrelated with the other effects.

To evaluate the various contributions to the overall uncertainty, σ_{C_D}, a reference transport configuration is chosen:

$M = 0.8 \quad Re = 3 \times 10^6$

$C_L = 0.6$

$C_{D_{C_{L=0}}} = 0.015$, parabolic drag polar

$\frac{\partial C_D}{\partial i_t}\frac{\ell_t}{C} = 0.003/\text{deg}$

$A = 12$

$e = 0.9$

$\frac{\partial C_D}{\partial M} = 0.1$ (drag divergence)

$\frac{S_{we}}{S} = 5.6 \quad \alpha = 4°$

$C_{D_{bc}} = 0, \quad \frac{A_{bc}\cos\alpha}{S} = -0.1$

Other assumptions in the evaluation are as follows:

Balance normal-force capacity, $F_{N_{des}}$, is twice the lift at cruise

Balance chord-force capacity, $F_{C_{des}}$, is 0.1 $F_{N_{des}}$

Balance axis aligned with body axis

Balance state of the art is 0.15% full scale

Balance operating at half design normal force

Pressure transducer state of the art is 0.05% full scale

Angle of attack sensor state of the art is $\sigma = 0.01°$

Temperature sensor state of the art $2\sigma = 0.01$ T

3.2 Discussion of Contributions

In order of appearance, the contributions considered are standard deviation in Reference Mach number, Normal Force, Chord Force, angle of attack, Reynolds number, Mach gradient, Flow Curvature, Upwash, Base pressure, Static pressure, and Internal Drag.

Reference Mach number —

$$\frac{\partial C_D}{\partial M} = \frac{\partial C_D}{\partial M_{\text{drag rise}}} - \frac{2C_D}{M} - \left(\frac{\partial C_D}{\partial C_L}\right)\left(\frac{2C_L}{M}\right)$$

The above expression (Ref. 11) is obtained by defining drag and lift coefficients (C_D and C_L) in terms of Normal and Chord force (F_N and F_C), angle of attack, and dynamic pressure; taking the derivative with respect to Mach number; and then substituting to eliminate dynamic pressure.

Presented in Fig. 2 is the contribution to drag,

$$\sigma_{C_{D_M}} = \frac{\partial C_D}{\partial M}\sigma_M$$

as a function of σ_M for a variety of C_L and Ae values. At the reference conditions, a $2\sigma_M$ of the order 0.005, which is frequently quoted as an overall precision/accuracy, produces a 2σ $C_{D_M} = 0.0001$. This correlates well with the widely accepted value of $\sigma_M = 0.0001$ (Table 1) as being necessary for the required precision/accuracy in drag.

Balance data accuracy —

$$\text{Normal force:} \quad \frac{\partial C_D}{\partial F_N} = \frac{\sin\alpha}{q_\infty S} + \frac{\partial C_D}{\partial C_L}\frac{\cos\alpha}{q_\infty S}$$

$$\text{Chord force: } \frac{\partial C_D}{\partial F_C} = \frac{\cos \alpha}{q_\infty S} - \frac{\partial C_D}{\partial C_L} \frac{\sin \alpha}{q_\infty S}$$

The following assumptions and conditions are imposed:

Parabolic drag polar $\frac{\partial C_D}{\partial C_L} = \frac{2C_L}{\pi A e}$

Standard deviation proportional to design load and $\sigma_{F_N} = \varepsilon F_{N_{des}}$

Chord-force design load = 0.1 normal-force design load $F_{C_{des}} = 0.1\ F_{N_{des}}$

Operating at 1/2 design condition $\sigma_{F_C} = \varepsilon F_{C_{des}}$

Reference angle of attack of 4° $\frac{F_{N_{des}}}{q_\infty S} \cong 2C_{L_{reference}} = 1.2$

Reference effective aspect ratio of 10.8

Then

$$\sigma_{C_{D_{F_N}}} = 0.126\varepsilon \quad \text{and} \quad \sigma_{C_{D_{F_C}}} = 0.12\varepsilon$$

which combines in the root-mean-square sense for equal ε to $\sigma_{C_{D_F}} = 0.174\varepsilon$. Typically, ε is such that $2\sigma F_N$ is about 0.15% $F_{N_{des}}$, which yields a $\sigma_{C_{D_F}} = 0.00019$. The results of the foregoing analysis are presented in Fig. 3 for $C_L = 0.6$ and $C_L = 0.4$.

Increasing the ratio of design load to operating load at constant C_L results in a linear increase in deviation. In order to achieve the required C_D accuracy of 0.0001 as stated in Table 1, the balance must be operated at design conditions and the standard deviation should be reduced by a factor of 2.

Angle of Attack —

$$\frac{\partial C_D}{\partial \alpha} = \left[C_L - \frac{\partial C_D}{\partial C_L} C_D \right]$$

For the reference conditions, $\partial C_D/\partial \alpha = 0.599$, which results in a $\sigma_\alpha = 0.0096°$, required to produce a $\sigma_{C_D} = 0.0001$. This corresponds to the 0.01° angle-of-attack figure presented in Table 1. Figure 4 is a plot of $\sigma_{C_{D_\alpha}}$ per 0.01° of σ_α as a function of C_L for a variety of aspect ratios.

Uncertainty in angle of attack is idealized as composed of stream angle and geometric effects:

$$(\sigma_\alpha)^2 = (\sigma_\alpha)^2_{\text{stream angle}} + (\sigma_\alpha)^2_{\text{geometric}}$$

The ability to determine stream angle seems to be limited by tunnel flow precision and balance accuracy. Accuracies are quoted in Ref. 1 to range from 0.01° to 0.04°. Stream angle determined from balance measurement results in

$$\sigma^2_{\alpha_{\text{stream angle}}} \cong \left(\frac{\sigma_{F_N}}{q_\infty S \dfrac{dC_L}{d\alpha}} \right)^2 + (\sigma_\alpha)^2_{\text{tunnel precision}}$$

choosing $dC_L/d\alpha = 0.1/\text{deg}$ and the reference conditions and assumed balance accuracy of 0.15% results in

$$\sigma^2_{\alpha_{\text{stream angle}}} = (.009°)^2 + (\sigma_\alpha)^2_{\text{tunnel precision}}$$

Assuming a tunnel precision of equal value leads to σ_α stream angle = 0.013°.

The accuracy of geometric angle-of-attack measurements varies widely, depending on the test environment and the method used. Most seem to produce a 2σ precision of the order of 0.05°. Modern laser technology application is leading toward a σ_α of 0.01°. Overall then, it seems more likely that a $\sigma_\alpha = 0.02°$ is achievable as opposed to 0.01°.

Reynolds number — Reynolds number effects on drag are idealized as resulting from skin-friction effects and from transonic effects (changes in pressure drag and wave drag from shock movement due to changes in boundary-layer thickness). Hence,

$$\frac{\partial C_D}{\partial Re} = \frac{\partial C_{D_f}}{\partial Re} + \frac{\partial C_{D_t}}{\partial Re}$$

Skin friction: Figure 5, which is taken from Ref. 12, shows that Prandtl-Schlichting, Karman-Schoenherr, Schultz-Grunow, and Winter-Gaudet methods of estimating turbulent skin friction are all comparable. Hence, for convenience, the Prandtl-Schlichting relationship

$$C_f = \frac{0.455}{(\log_{10} Re)^{2.58}}$$

is differentiated to produce

$$\frac{dC_f}{C_f} = \frac{-2.58(\log_{10} e)}{(\log_{10} Re)} \frac{dRe}{Re}$$

Assuming a form factor correction to wetted area,

$$\frac{\partial C_{D_f}}{\partial Re} = \frac{-0.5098}{Re(\log_{10} Re)^{3.58}} \frac{S_{we}}{S}$$

The results of this equation are presented in Fig. 6. At the reference conditions, $\sigma_{Re} \cong 100{,}000$ results in $\sigma_{C_{D_f}} \cong 0.0001$. On this basis, a $\sigma_{Re} = 100{,}000$ is suggested as the criterion for forming estimates of other related criteria.

Transonic effects: The effects of Reynolds number on transonic effects should be found from experiment, because transonic behavior will differ for each model and also for boundary-layer transition. For example, as presented in Fig. 7, numerical results for a modified version of the Whitcomb 1202-4 airfoil with both fixed and free transition show quite different behavior.

Other effects: Not previously discussed is the effect Reynolds number has on angle of zero lift. Reference 13 shows that the free-transition results for the C-SA correlation are particularly affected, varying by 0.3° over the Reynolds number range from 1.75×10^6 to 4.2×10^6, whereas, fixed-transition results vary only by 0.03° for the same range.

Transition Reynolds number has clearly been shown to be affected by noise in the airstream. The method of Benek and High (Ref. 14) correlates well with experimental results from the AEDC 16T facility. The well-known AEDC 10° cone results from numerous tunnels (Ref. 15) show that transition is strongly dependent on noise. Results from tests of this cone are presented in Fig. 8 (Ref. 16) for Mach number 0.8. The results of the C-5A wind-tunnel correlation (Ref. 13), showed that best agreement was achieved when the differences in transition Reynolds number were assumed to represent a transonic turbulence factor, and a correction for Reynolds number was applied accordingly. This seems to be counter to the information presented in Sec. 2.3. The conflict may be resolved by noting that the boundary layer on the model was largely transitional or very early turbulent. The issue is by no means closed. With the assumption that for wind-tunnel models the effect is valid, $Re = 100{,}000$ results in a $\langle p' \rangle / q_\infty$ of ≈ 0.001 for negligible effect which is over an order of magnitude less than the 2% value noted in Sec. 2.3.

Correlation of the Preston-tube data from the Ames 11-Foot Transonic Wind Tunnel (Ref. 16) and flight-test results (Ref. 17), as well as comparison of unit Reynolds numbers for the same C_f, probe pressure, and effective probe height, shows approximately a 6% greater effective Reynolds number in the tunnel for laminar boundary-layer development (Fig. 9). These results are not conclusive, but they do serve to illustrate the potential problem. Work in this area is needed.

Mach gradient — The longitudinal gradient in static pressure is a recognized source of drag that must be taken into account. The more accurate method is to integrate the static-pressure coefficient distribution as a function of A_n/S to evaluate the $C_{D_{buoyancy}}$ term. A discussion of this is provided in Ref. 2, which references earlier work by Isaacs (Ref. 18) and Morris and Winter (Ref. 19). As pointed out in Ref. 2,

$$C_{D_{buoyancy}} = C_{D_{\frac{dM}{dX}}}$$

can be idealized as

$$\frac{C_{D_{\frac{dM}{dX}}}}{} = \frac{V}{SL}\left[\frac{10}{M(5 + M^2)}\right] \frac{dM}{d\frac{X}{L}}$$

Here, the term $dM/[d(X/L)]$ represents the change in Mach number over the length of the model (L). Presented in Fig. 10 is the contribution of $dM/[d(X/L)]$ to C_D as a function of Mach number for a range of V/SL values. As can be seen in the figure, at $M = 0.8$, a change in Mach number over the length of the model of less than 0.001 produces a $C_{D_{buoyancy}} = 0.0001$.

Since the slope of the curve is nearly constant with Mach number, the criterion of $\{dM/[d(X/L)]\}/M = 0.06\%$ is suggested for Mach gradient. For transonic conditions, this is within the allowable $\Delta M = 0.001$ as presented in Table 1. Uncertainty of $\sigma_{dM/[d(X/L)]} = 0.0006M$ would also represent an uncertainty in buoyancy of $\sigma_{C_{D_{buoyancy}}} = 0.0001$.

Stream curvature — Induced camber and induced tail incidence are two principal effects of flow curvature:

$$\sigma_{C_D}{}_{\text{stream curvature}} = \left[\frac{\partial C_D}{\partial_{\text{camber}}} + \frac{\partial C_D}{\partial_{\text{tail incidence}}}\frac{\ell_t}{C}\right]\frac{d\frac{W}{u_\infty}}{d\frac{X}{C}}$$

Induced camber: At transonic speeds, the drag rise characteristics are particularly affected. Each user of a given facility should assess the effect for this configuration. As an example, presented in Fig. 11 is the result of computations of a 1202.4 airfoil at $M = 0.78$ with circular-arc camber added. A $\Delta y/C = 0.000125(X/C)(1 - X/C)$ produces a ΔC_D shock of 0.00005, which is equivalent to a stream angle change of 0.00025 rad in one chord lengh = 0.014 deg/chord. Certainly, away from these conditions, the influence will be significantly less. Based on this limited analysis, it is suggested that the desired accuracy, at or near design, be 0.03 deg/chord.

Tail incidence: Tail incidence owing to flow curvature affects trim drag:

$$\sigma_{C_{D_t}} = \frac{\partial C_D}{\partial i_t}\frac{\ell_t}{C}\frac{d\frac{W}{u_\infty}}{d\frac{X}{C}} = \frac{\partial C_D}{\partial i_t}\sigma_{i_t}$$

Presented in Fig. 12 is the result of the above equation for $\sigma_{C_{D_t}} = 0.0001$ as a function of ℓ_t/C. Estimating $\partial C_D/\partial i_t(\ell_t/C)$ to be $\cong 0.003$/deg, $d(W/u_\infty)/d(X/C)$ of the order of 0.0006 is seen to result in $\sigma_{C_{D_t}} = 0.0001$. From the standpoint of trim drag, $d(W/u_\infty)/d(X/C) = 0.0006$ is suggested as the criterion for flow curvature. This is equivalent to 0.034°/chord, which compares favorably with the 0.03 deg/chord criterion suggested for induced-camber effects.

Stream upwash — The effect of the mean value of stream upwash is contained in the discussion of Sec. 3.2.3, Angle of Attack. The mean upwash at zero lift is the tunnel stream angularity. The mean upwash owing to lift interference is treated as an addition to the geometric angle-of-attack term. Remaining is the effect spanwise variation of upwash has on the drag polar shape. Sources of this variation are wall interference and swirl in the tunnel flow field. As a measure of the significance of this flow, a wing having an elliptical lift distribution is compared to a wing with an elliptical lift plus a parabolic added-lift distribution.

The analysis is after the method of Glauert which is outlined in the appendix to Ref. 20.

Basic elliptical lift

$$\left[\frac{C_\ell \frac{c}{c_{ave}}}{C_{\ell_o}\frac{c_o}{c_{ave}}}\right]^2 + \left[\frac{2y}{b}\right]^2 = 1$$

plus the parabolic increment

$$\Delta C_\ell \frac{c}{c_{ave}} = \delta \frac{c_o}{c_{ave}}\left[1 - \left(\frac{2y}{b}\right)^2\right]$$

which produces lift for elliptic loading

$$C_{L_e} = \frac{\pi}{4}\left(C_{L_{o_e}}\frac{c_o}{c_{ave}}\right)$$

and for elliptic + parabolic loading

$$C_{L_{e+p}} = \frac{\pi}{4} C_{\ell_{o_{e+p}}}\frac{c_o}{c_{ave}}\left(1 + \frac{8\delta}{3\pi}\right)$$

Holding C_L constant requires variation in angle of attack and corresponding C_ℓ:

$$\frac{C_{\ell_e}}{C_{\ell_{e+p}}} = \frac{\alpha_e}{\alpha_e + \Delta\alpha} = \frac{1 + \frac{8\delta}{3\pi}}{1 + \delta\left(1 - \frac{4y^2}{b^2}\right)^{1/2}}$$

which results in

$$\frac{\Delta\alpha}{\alpha_e} = \frac{1 + \delta\left(1 - \frac{4y^2}{b^2}\right)^{1/2}}{1 + \frac{8\delta}{3\pi}} - 1$$

Based on the Fourier analysis of the lift distributions:

$$C_{D_{i_{e+p}}} - C_{D_{i_e}} = \frac{C_L^2}{\pi A} \frac{64\delta^2}{\left(1 + \frac{8\delta}{3\pi}\right)^2} \sum_{n=3.5}^{\infty} \frac{1}{n(n^2 - 4)^2}$$

For the reference conditions, $A = 12$ and $C_L = 0.6$ $\delta = 0.1$ results $\Delta C_{D_i} = 0.00007$. With this variation, $\Delta\alpha/\alpha$ at the root section is 1.4% higher and at $\eta = 0.95$ is 6% lower. For a wing taper ratio 2 and average section lift coefficient slope of 0.1/deg, this variation will increase α at the root by 0.08° and decrease α at $\eta = 0.95$ by 0.6°. The variation in $\Delta\alpha/\alpha$ as a function of η is presented in Fig. 13.

By way of comparison, the effect of varying wing incidence on the outer portion, along the span of a modern transport configuration, is shown in Fig. 14. A maximum variation of $\Delta\alpha = 0.4°$ produces a $\Delta C_D = 0.0002$. This computation was performed for a nominal C_L of 0.45, using a vortex-lattice approach. The results are comparable and serve to illustrate that the outer span flow is most critical. Models with large span-to-tunnel-width ratio (exceeding about 0.6) will be particularly affected by tunnel-wall upwash interference varying along the span (Ref. 21).

From the foregoing, to hold $\sigma_{C_{D_i}}(w/u_\infty)$ under 0.0001, it is suggested that the spanwise variation in stream angle + lift interference be defined within ±0.1°.

Model base and cavity pressure — For either base or cavity pressure, uncertainty stems from the measurement error associated with static and total pressure error. The uncertainty is the same, hence

$$C_{D_{bc}} = \left(\frac{P_{bc} - P_\infty}{q_\infty S}\right) A_{bc} \cos\alpha$$

Then

$$\left(\sigma_{C_{D_{bc}}}\right)^2 = \left[-C_{D_{bc}}\left(\frac{5M - 10}{7M^2}\right) - \frac{10}{7M^2}\frac{A_{bc}}{S}\cos\alpha\right]^2\left(\frac{\sigma_{P_\infty}}{P_\infty}\right)^2$$

$$+ \left[-2C_{D_{bc}}\left(\frac{5 + M^2}{7M^2}\right)\right]^2\left(\frac{\sigma_{P_t}}{P_t}\right)^2 + \left[C_{D_{bc}} + \frac{10A_{bc}\cos\alpha}{7M^2S}\right]^2\left(\frac{\sigma_{P_{bc}}}{P_{bc}}\right)^2$$

At or near $C_{D_{bc}} = 0$, and expressing $\sigma_P = \varepsilon P$, then

$$\sigma_{C_{D_{bc}}} \cong \varepsilon 2\sqrt{2}\,\frac{10}{7M^2}\frac{A_{bc}}{S}\cos\alpha$$

A transducer of $\varepsilon = 0.001$ is typical. Presented in Fig. 15 is the deviation, σ_{C_D}, due to $\varepsilon = 0.001$, as a function of Mach number for a variety of $(A_{bc}/S)\cos\alpha$. For the reference transport conditions, $\sigma_{C_{D_{bc}}} = 0.00006$. For $C_{D_{bc}} = 0.001$, the result is $\sigma_{C_{D_{bc}}} = 0.000061$. Missile configurations are more sensitive since $A_{bc}/S = 1.0$. At $M = 0.8$, $C_{D_{bc}} = 0$, $\alpha = 0$, $\sigma_{C_{D_{bc}}}$ for a missile = 0.0063.

Pressure and temperature requirements — Uncertainty requirements for pressure and temperature measurements are dictated by the requirements for uncertainty of Mach number and Reynolds number.

Pressure: Defining

$$\sigma_M^2 = \left[\frac{\partial M}{\partial P_{t_\infty}}\sigma_{P_{t_\infty}}\right]^2 + \left[\frac{\partial M}{\partial P_\infty}\sigma_{P_\infty}\right]^2 \quad \text{and} \quad \sigma_P = \varepsilon P_{fs}$$

$$\frac{\partial M}{\partial P_{t_\infty}}\sigma_{P_{t_\infty}} = \left[\frac{M^2 + 5}{7M}\right]\frac{\varepsilon P_{t_{fs}}}{P_{t_\infty}}$$

$$\frac{\partial M}{\partial P_\infty}\sigma_{P_\infty} = -\left[\frac{M^2 + 5}{7M}\right]\frac{\varepsilon P_{fs}}{P_\infty}$$

The result of these equations is presented in Fig. 16.

At Mach number 0.8, an ε of 0.0005 (which is representative of the current technology) produces a σ_M of 0.0005 for both P_{t_∞} and P_∞, which results in an overall σ_M of 0.0007.

Table 1 indicates $\Delta C_p = 0.001$ for small configurational changes. This is equivalent to $\varepsilon \cong (7/10)M^2\Delta C_p = 0.0005$ at Mach 0.8.

Temperature: Using the expression for Re,

$$Re = (2.29 \times 10^6)\ell_{meters} \frac{P_{t_\infty} M}{T_o^2(1 + 0.2M^2)^{1.5}} \left(\frac{T_o}{1 + 0.2M^2} + 110.3\right)$$

and noting that $M = M(P_{t_\infty}, P_\infty)$

$$\sigma_{Re} = \left\{\left[\frac{\partial Re}{\partial P_{t_\infty}} \sigma_{P_{t_\infty}}\right]^2 + \left[\frac{\partial Re}{\partial P_\infty} \sigma_{P_\infty}\right]^2 + \left[\frac{\partial Re}{\partial T_o} \sigma_{T_o}\right]^2\right\}^{1/2}$$

$$\frac{\partial Re}{\partial P_{t_\infty}} \sigma_{P_{t_\infty}} = \frac{5}{7} Re\left[1 + \frac{1}{M^2} - \frac{2}{5 + \frac{110.3}{T_o}(5 + M^2)}\right] \frac{\sigma_{P_{t_\infty}}}{P_{t_\infty}} \tag{1}$$

$$\frac{\partial Re}{\partial P_\infty} \sigma_{P_\infty} = \frac{Re}{7}\left[2 - \frac{5}{M^2} + \frac{10}{5 + \frac{110.3}{T_o}(5 + M^2)}\right] \frac{\sigma_{P_\infty}}{P_\infty} \tag{2}$$

$$\frac{\partial Re}{\partial T_o} \sigma_{T_o} = -Re\left[1 + \frac{(5+M^2)\frac{110.3}{T_o}}{5+\frac{110.3}{T_o}(5+M^2)}\right] \frac{\sigma_{T_o}}{T_o} \tag{3}$$

The combined effects of $\sigma_{P_{t_\infty}}$ and σ_{P_∞} from Eqs. (1) and (2) are presented in Fig. 17 as a function of Mach number for $T_o = 100°K$ and $300°K$. At Mach number 0.8, σ_{Re} is of the order of 0.15% of Re per 0.1% of pressure deviation. Comparing this with the criterion of $\sigma_{Re} = 100{,}000$, it is seen that the uncertainty of measurement from modern pressure transducers is not a significant factor at Re less than 50×10^6. Presented in Fig. 18 is the deviation in Re due to a 1% deviation in T_o as a function of Mach number. A 1% deviation in T_o results in 1.3% deviation in Re at Mach number 0.8. At moderate Reynolds number, up to about 8×10^6, the criterion of $\sigma_{Re} = 100{,}000$ results in $\sigma_{T_o}/T_o = 1\%$ being sufficient. This means that conventional facilities represented by $T_o = 311°K$ having a σ_{T_o}, including temperature spottiness, of 30°C would satisfy reasonable requirements for data uncertainty and flow quality.

Internal drag — There are many ways of defining and determining duct losses. The key to all of them is an accurate determination of weight flow. References 22 through 24 contain information on this subject, as well as the related subject of testing for powered-nacelle effects. In general, whether for rakes, a venturi, calibrated orifices, or exit plugs, some sort of weight-flow calibration is required. One approach (R. Bengelink, Boeing, Seattle, private communication) to performing duct loss calibrations is to define internal drag, D_{int}, as

$$D_{int} = (1 - C_v)\frac{\dot{W}}{g} V_{ideal}$$

where

$$C_v = \frac{F_{balance}}{\frac{\dot{W}}{g} V_{ideal}} \quad \text{and} \quad V_{ideal} = \left\{7gRT_{t_\infty}\left[1 - \left(\frac{P_{t_\infty}}{P_\infty}\right)^{-2/7}\right]\right\}^{-1/2}$$

$F_{balance}$ and $\dot{W}$ are obtained in a calibration facility. In the calibration facility, $\dot{W}$ is determined from a system of venturis that includes instrumentation of high precision and accuracy. With such a system $\sigma_{\dot{W}V_{ideal}}/\dot{W}V_{ideal}$ is of the order 0.001. Correspondingly, $F_{balance}$ has a σ_F/F of the order of 0.001. With these deviations, C_v as calibrated has a deviation owing to the measurement deviations of

$$\frac{\sigma_{C_v}}{C_v} = \left\{\left[\frac{\sigma_F}{F}\right]^2 + \left[\frac{\sigma_{\dot{W}V_{ideal}}}{\dot{W}V_{ideal}}\right]^2\right\}^{1/2} = 0.0014$$

in the wind tunnel

$$C_{D_{int}} = (1 - C_v)\frac{\dot{W}}{g}\frac{V_{ideal}}{q_\infty}$$

On the basis of the definition of C_v, and $C_{D_{int}}$, and recognizing that V_{ideal} and q_∞ are both functions of P_{t_∞} and P_∞, the various components contribute as follows: typical value for high-bypass flow-through nacelles is $C_v \cong 0.95$. For this condition, the contribution to $\sigma_{C_{D_{int}}}/C_{D_{int}}$ owing to σ_{C_v}/C_v is

$$\left(\frac{1}{\frac{1}{0.95} - 1}\right)\frac{\sigma_{C_V}}{C_V} = \frac{19\sigma_{C_V}}{C_V}$$

The calibrated orifice, or rake used to measure $\dot{W}$, was calibrated using a suction tank with essentially no airflow around the model. In the tunnel, the inlet airflow is considerably more distorted than in the tank because of the high-velocity external flow field. It is safe to assume that $\sigma_{\dot{W}}/\dot{W}$ is considerably larger than in the calibration facility. Depending on the nacelle installation and configuration, the value of $\sigma_{\dot{W}}/\dot{W}$ may range from 0.001 to 0.01 or more. For the reference transport configuration, a value of 0.002 is assumed. For high-quality resistance temperature transducers, precision is of the order of $2\sigma_{T_{t_\infty}} = 0.05\%$ full scale.

Customarily, T_0 is not measured in the duct, but is the result of a temperature survey of the tunnel; hence, the overall uncertainty is of the order of 3°C. Assuming a bias of 1.5°C and a 2σ precision of the tunnel of 1.5°C, then for $T_0 = 311°K$,

$$\frac{\sigma_{T_{t_\infty}}}{T_{t_\infty}} = \frac{0.75}{311} = 0.0024$$

which is approximately an order of magnitude less precise than the precision of the high-quality temperature transducer. Representative 2σ deviation for commercially available pressure transducers is 0.10% full scale. Assuming that pressure transducers used to determine P_{t_∞} and P_∞ are used appropriately, $\sigma_{P_{t_\infty}}/P_{t_\infty}$ and $\sigma_{P_\infty}/P_\infty$ are assumed to be 0.005. Assuming a reference Mach number of 0.8, and substituting these results in the expression for $\sigma_{C_{D_{int}}}/C_{D_{int}}$

$$\frac{\sigma_{C_{D_{int}}}}{C_{D_{int}}} = \left\{[19(0.0014)]^2 + (0.002)^2 + \left[\frac{1}{2}(0.0024)\right]^2 + \frac{1}{49}(9.8)^2[(0.005)^2 + (0.005)^2]\right\}^{1/2} = 0.02$$

For high-bypass separate-flow nacelles, $C_{D_{int}}$ ranges from about 0.0006 to 0.0012. With this range, the deviation in $C_{D_{int}}$ for, say, a twin-nacelle installation is of the order of $\sigma_{C_{D_{int}}} = 0.00007$ or less. In other situations wherein rakes are typically used and in which the internal drag may be quite high, such as in a fighter-type configuration, weight flow $\dot{W}$ may be much more in error, and the internal drag uncertainty could be an order of magnitude more than the above. An assessment of the uncertainty, based on the method used to acquire and reduce the data is necessary to defining the actual level of uncertainty.

Humidity — It is generally accepted that condensation is to be avoided. A highly conservative approach is for the dew-point temperature to be below that corresponding to the highest local Mach number of the flow over the model. Because of factors such as lag time in the heat-transfer process resulting in condensation and supersaturation, this is unnecessarily restrictive. Experience shows that a dew point at or below that corresponding to the free-stream static temperature is sufficient to avoid condensation. Hence, to avoid condensation, a criterion of the dew point being 2°C below free-stream static temperature is suggested.

As will be shown in the following, the effects of humidity, in the form of water vapor, on the gas constant γ are insignificant for easily obtainable humidity levels. Air is idealized as a mixture of oxygen and nitrogen, and the following thermodynamic properties at 25°C are chosen as representative:

		C_p, cal/mole C	C_V, cal/mole C	Molecular weight, g/mole
O_2	1.3925	7.05	5.063	32
N_2	1.4012	6.94	4.953	28
H_2O	1.505	5.92	3.933	18

Then, with the O_2 mole fraction = 0.205, γ air = 1.39954 and γ air + water at 0.001 relative humidity = 1.39967 results in $\Delta\gamma/\Delta_{\text{relative humidity}} = 0.13$. From

$$\frac{P_{t_\infty}}{P_\infty} = \left(1 + \frac{\gamma - 1}{2}M^2\right)^{\gamma/\gamma-1} \quad \text{for} \quad \gamma = \frac{7}{5}$$

$$\frac{dP_{t_\infty}}{P_{t_\infty}} - \frac{dP_\infty}{P_\infty} = \left(\frac{35}{4}\frac{M^2}{5 + M^2} - \frac{25}{4}\ln\frac{5 + M^2}{5}\right)d\gamma + \frac{7M}{5 + M^2}dM$$

At constant pressure,

$$\frac{dM}{d\gamma} = -\left[\frac{5}{4}M - \frac{25}{28M}(5 + M^2)\ln\frac{5 + M^2}{5}\right]$$

In the transonic range from $M = 0.6$ to $M = 1.4$, $dM/d\gamma$ ranges from -0.195 to -0.282. With this range of values, the humidity corresponding to $\Delta M = -0.001$ is $\geq 0.001/0.195(0.13) = 0.039$. Since humidity levels in transonic tunnels are typically below 0.001, it is seen that humidity affecting γ is not a problem. Therefore, any flow-quality criteria for humidity should be based on condensation. Having met the suggested criteria, the effect of humidity on the measurements, and on drag in particular, should be negligible.

3.3 Summary of Deviation Effects

For the reference transport at $M = 0.8$, the following conditions are assumed:

$$\frac{\partial C_D}{\partial M} = 0.1 \ , \quad C_L = 0.6 \ , \quad Ae = 10.8 \ , \quad \frac{Swe}{S} = 5.6$$

$$\frac{A_{bc}}{S} = 0.02 \quad Re = 4 \times 10^6$$

Further, assuming the deviations as presented in the discussion, Relative Magnitude of Bias and Deviation, from the preceding analysis and discussion, the 1σ's are as follows:

$$\sigma_{C_{D_M}} = 0.00005 \ (2\sigma_M = 0.005) \qquad \sigma_{C_{D_{curvature}}} = 0.00003 \left(\frac{d\alpha}{d\frac{x}{c}} \leq 0.03°\right)$$

$$\sigma_{C_{D_F}} = 0.00013 \qquad \sigma_{C_{D_{bc}}} = 0.00003$$

$$\sigma_{C_{D_{Re}}} = 0.00002 \left(\frac{2\sigma_{T_o}}{T_o} = 0.01\right) \qquad \sigma_{C_{D_{int}}} = 0.00005$$

$$\sigma_{C_{D_\alpha}} = 0.0001 \ (\sigma_\alpha = 0.01°) \qquad \sigma_{C_{D_{\frac{dM}{d\frac{x}{\ell}}}}} \text{ assumed to be negligible}$$

$$\sigma_{C_{D_{twist}}} = 0.00003 \left(\frac{d\alpha}{d\eta} \leq 0.1°\right)$$

which combines to give an overall $\sigma_{C_D} = 0.00019$. For a composite root-sum standard deviation of $\sigma_{C_D} = 0.00019$ and from the rough estimate of the relative magnitude of bias and deviation error, the total uncertainty at the 95% confidence level is ± 0.0008 in C_D.

4. OTHER TYPES OF MEASUREMENTS

4.1 Laminar Flow Control Technology

The development of laminar flow control (LFC) technology in the wind tunnel places the most severe requirement on the aero-noise quality because of the dominance of external disturbances on the stability of laminar boundary layers. It has been shown earlier that the magnitude of local boundary-layer suction flow required to maintain laminar flow increases with induced high sound intensities (Refs. 25,26). Air particle fluctuations caused by impinging sound waves add to the displacements caused by flow turbulence, and the resulting disturbances undergo the well-known Tollmien-Schlichting and cross-flow amplifications as these disturbances propagate in the boundary layer, that is, boundary-layer receptivity (Morkovin). The amplifications of these growth disturbances have been shown experimentally (Ref. 25) and theoretically (Ref. 27) to occur only for fluctuating disturbances in a limited frequency range corresponding to the Tollmien-Schlichting and cross-flow spectral regions over a given wing design.

Utilizing measured disturbance levels in the NASA/LRC-8-ft TPT (Ref. 19) and the critical boundary-layer instability modes on the NASA LRC developed swept super critical LFC airfoil (Refs. 27-29), reduction in SPL with frequency was determined for the LRC TPT test section to prevent transition on the wing. Figure 18 shows the existing SPL with slots closed compared with that desired for $M = 0.8$. The desired distribution of SPL is based on calculations of T - S and cross-flow instabilities over the wing upper surface using conservative incompressible stability analysis (Ref. 27). These calculations limited the maximum growth disturbance amplitude ratio ($n = \ell n \, A/A_o$) to about 4.5 in the nose region, 6.5 in the mid-chord region, and 7 in the aft wing region for design. Figure 19 shows the required SPL reduction with frequency relative to the existing level to prevent transition at $M = 0.8$. From a similar approach estimates were made to determine the critical SPL for $0.2 \leq M \leq 1.0$, as shown in Fig. 20 compared with existing levels with and without slots closed. Figure 21 shows the critical SPL level with frequency for the LPC swept wing design at $M = 0.8$ and $Re/ft = 3 \times 10^6$. The solid curve is based on analysis of the swept wing. The dashed curve illustrates critical values of SPL that may be established by possible unstable modes involving slowly moving streamwise vortices, that is, upstream turning were support generated vortices.

Figure 22 shows the maximum chord Reynolds number with LFC and with turbulence level for low drag wings and bodies of revolution and flight results. The various tunnel data for maximum Re or transition are for $0 < M < 0.3$ and illustrate the influence of characteristic broad-based disturbance on transition. The flight data are influenced by propulsion- and fuselage-generated disturbances. The indicated LFC wing design point was partly based on the previously discussed approach and criteria and it was verified that the required level of $u'/U_\infty \leq 0.05\%$ was achievable utilizing a sonic throat (Ref. 30). With the addition of scheduled LRC/8' TPT modifications (HC + screens), it is expected that the level can be reduced to $u'/U_\infty \approx 0.02$-0.03% for transonic speeds. It is suggested that the criteria of $u'/U_\infty = 0.05\%$ be established for LFC development.

4.2 Determination of Boundary-Layer Properties by Holographic Methods

The technology for holographic measurement of boundary-layer properties by optical methods is rapidly advancing. The measurements are limited by both the quality of the optics and the quality of the airstream. Airstream, density fluctuations $\langle \rho' \rangle$ (denotes root mean square of the time-dependent density perturbation)

affect the quality. The effect of $\langle\rho'\rangle$ is to distort the wavefront of the signal at the focal plane of the receiving optics which results in noise superimposed on the true signal. The greater the optical path length, the greater the distortion. The conventional means of identifying the quality of the flow is the distortion length σ (termed optical aberration). The distortion length σ is defined from the following relation:

$$\sigma^2 = 2(G.D.)^2 \int_0^L \langle\rho'\rangle^2 \ell_x \, dx$$

where G.D. is the Gladstone-Dale constant (0.000227 M^3/kg), L is the optical path length, and ℓ_x is the integral spatial correlation of $\langle\rho'\rangle$ between two points along the optical path. The integral spatial correlation ℓ_x is usually found from cross-correlation of hot-wire measurements taken at different points along the path length.

Reference 31 contains numerous reports on the subject of aero-optics. The results of airborne measurements of atmospheric turbulence by Rose and Otten are presented in this publication. For example, at Mach 0.83 at an altitude of 8.84 km, $\langle\rho'\rangle/\rho_\infty = 0.019\%$ and $\ell_x \cong 7.1$ m, which for light of $\lambda = 0.63$ μm produced a $\sigma/\lambda_{0.63\ \mu m}$ of 3.9/km ($\sigma/\lambda L_{0.63} = 0.0039$/m), and $\lambda = 10.6$ μm results in

$$\frac{\sigma}{\lambda_{10.6\ \mu m}} = 0.23 \left(\frac{\sigma}{\lambda L}_{10.6} = 0.00023/m\right)$$

Rose, Craig, and Raman have recently obtained measurements of the boundary-layer properties in the shear layers of separated flow from a bluff-body model installed in a 14-foot wind tunnel (Ref. 32). Values of $\sigma/\lambda L_{0.69}$ ranged from 5 to 10. Rose estimates that $\sigma/\lambda L$ for attached turbulent boundary layers might be as low as 10% of the shear-layer value. The requirements for flow quality for these types of measurements is driven by the loss of confidence in the data that results from aero-noise (quantified by signal-to-noise ratio, S/N)

$$\frac{\sigma_{data}}{\sigma_{tunnel}} \cong S/N = \left[\left(\frac{\sigma}{L\lambda}\right)_{data} L_{data}\right]\left[\left(\frac{\sigma}{L\lambda}\right)_{tunnel} L_{tunnel}\right]$$

where L_{data} is proportional to model size and L_{tunnel} is proportional to tunnel size. Examining the relationship leads to the obvious conclusion that the model needs to be as large as possible and the optical path length as short as possible to achieve the maximum S/N. Further, for thin layers, it is easy to see why 2D testing is preferable (if not the only way) with the path parallel to the model. Then (neglecting side-wall effects) $L_{data}/L_{tunnel} = 1.0$. As an example, for thick shear layers, with $L_{data}/L_{tunnel} = 0.01$, $\sigma/L\lambda = 5$ and a limit on $S/N = 10 = [5/(\sigma/L\lambda)_{tunnel}](0.01)$ results in a desired $\sigma/L\lambda_{tunnel} = 0.005$. This is close to but higher than the free-air value. Presumably, treatment of the tunnel to reduce the scale length of $\langle\rho'\rangle$ (screens, honeycomb, high contraction ratio) could be done to achieve this.

In summary, the experimenter will have to evaluate the experiment/tunnel compatibility for himself. Determination of $\langle\rho'\rangle$ and ℓ_x as a function of tunnel conditions for each facility in question is necessary for proper assessment.

4.3 Desirable Particulate in the Flow Field for Laser Velocimetry

Since laser velocimetry depends on detecting Doppler frequency shifts owing to moving centers of light scattering, particulate matter in the flow field is welcome, provided that it is of the right type, size, and concentration. There are numerous references on the subject of laser velocimetry. Reference 33 is a compendium of laser instrumentation reports; it includes references dating from 1970. Reference 2 cites references from 1965 to 1976 and contains a considerable discussion of the subject. In particular, Ref. 2 contains a discussion of errors induced by particle lag. In that discussion, particles are idealized as obeying Stoke's law for drag. With this assumption, the equation of motion of a spherical particle in fluid flow is idealized by neglecting terms associated with density of the gas, ρ_g. The result is

$$\frac{(d_p)^2 \rho_p}{18\ \mu_g} \frac{dV_p}{dt} = (V_g - V_p)$$

The term on the right represents the lag in particle velocity from the velocity of the gas.

Assuming sinusoidal motion of the gas, the particle response is

$$\frac{V_p}{V_g} = \frac{1}{\left\{\left[\frac{(d_p)^2 \rho_p}{18\ \mu_g}\right]^2 \omega^2 + 1\right\}^{1/2}}$$

where ω is the gas motion (radians per second). This form is not entirely suitable for low-density flows. Other researchers (see Ref. 1) add a correction to account for the situation in which the mean free path ℓ is significant in relation to particle diameter dp. In this case, $[(d_p)^2\rho_p]/18\ \mu_g$ is replaced by $[(d_p)^2\rho_p]/18\ \mu_g[1 + \kappa(\ell/d_p)]$ where κ is the Cunningham constant (1.8 for air).

Figure 23 (Fig. A.11.5 in Ref. 2) is a solution for V_p/V_g (neglecting the Cunningham correction) for Mach number 1.0 conditions at 40°C stagnation temperature with $\rho_p = 1$ g/cm³ (representative of particulates such as oil vapor and smoke particles. Illustrated in the figure is the importance of particulate in the submicron size range. It is not obvious, but too small a particulate is essentially the same as no particulate and hence seeding of the flow would be required. Dennis A. Johnson (NASA Ames Research Center, private

communication) indicates that 0.3 μm to 0.7 μm is the desired range of particulate size and recommends the criterion that the number density C of particles in the range $C_{0.3\to0.7\ \mu m}$ be three orders of magnitude greater than the number density of particles of larger size, $C_{>0.7\ \mu m}$, that is,

$$\frac{C_{0.3\to0.7\ \mu m}}{C_{>0.7\ \mu m}} \geq 10^3$$

The desired number density of particles in the $C_{0.3}$ to $C_{0.7\ \mu m}$ range can be estimated from the relationship, data rate, $\dot{n}$, is approximated by $\dot{n} = CAV$. Here, A is the probe volume cross section and V is the velocity. Rearranging, $C = \dot{n}/AV$. In order to take data at a reasonable rate, $\dot{n}$ should be of the order of 10^3/sec to 10^5/sec. Assuming a probe volume cross section of (0.01 cm)(0.01 cm) and Mach number = 0.9 ~ 300 m/sec, substitution produces

$$\frac{10^3}{10^{-4}3\times10^4} \leq C \leq \frac{10^5}{10^{-4}3\times10^4} \quad \text{or} \quad \frac{333}{cm^3} \leq C \leq \frac{33{,}300}{cm^3}$$

Of course, choosing a different set of variables will result in different desired particulate concentrations. The researcher should determine these for the experiment in question.

4.4 Tunnel Cleanliness

It is difficult to quantify the effects of flow contaminants in the wind-tunnel airstream. Flow contaminants have the potential to affect model aerodynamic characteristics and to damage either the model or test instrumentation. There are no known criteria related to the effects of flow contaminants on model aerodynamic characteristics. However, models have been sandblasted to such an extent that boundary-layer transition moved to the leading edge, thereby simulating to some degree high-Reynolds-number conditions.

For tests associated with boundary-layer transition or laminar flow control such events are considered disastrous. As these special tests become more important, some criteria for tunnel cleanliness will have to be developed. Although the study of tunnel operational procedures is beyond the scope of this work, some criteria do exist for avoiding model or instrumentation damage. One such criterion, which is used at AEDC, is that a 0.25-in.^{2} surface area experience fewer than 60 particle hits per hour of operation at a dynamic pressure of 1000 lb/ft^2. Although particle size is not considered in this criterion and a target hit count is required, it has proved effective in preventing model and instrumentation damage.

5 SUMMARY OF FLOW-QUALITY AND DATA-ACCURACY REQUIREMENTS

The most stringent requirements for flow quality and data accuracy included in this paper are given below.

5.1 Flow Quality

Item	Description	Value	Basis
w/U_∞	Flow angle	≤0.01°	C_D = 0.0001
$[d(w/U_\infty)]/[d(x/c)]$	Flow curvature	≤0.03°/chord	C_D = 0.0001
$[d(w/U_\infty)]/d\eta$	Spanwise variation in flow angle	≤0.1°	C_D = 0.0001
$dM/[d(x/\ell)]$	Mach gradient	≤0.0006 M	C_D = 0.0001
u'/U_∞	Vorticity	≤0.0005	Laminar flow
$\langle p'\rangle/q_\infty$	Noise	≤0.0005	Laminar flow
ΔT	Temperature spottiness	±1°K	Boundary-layer study
ΔP_t	Total head variation	±0.002 P_t	Boundary-layer study
ΔP	Static pressure variation	±0.002 P	Boundary-layer study
$\sqrt{nF(n)}$	Disturbance frequency content	≤0.002	Flutter
$T-T_D$	Dewpoint temperature margin	2°C	Condensation
	Density fluctuation and integral spatial correlation of p'	Experiment dependent	Signal/noise ratio
d_p	Particulate diameter	0.3 to 0.7 m	Signal and particle lag for LV work
C	Number density of particles	333/ to 33,300/3	Signal and particle lag for LV work

5.2 Data Accuracy

Item	Description	2 Value	Basis
Po	Stagnation pressure	0.001 P_{fs}	C_D = 0.0001
P	Static pressure	0.001 P_{fs}	C_D = 0.0001
To	Stagnation temperature	0.01 To	C_D = 0.0001
M	Mach number	0.0002	C_D = 0.0001
	Angle of attack	0.01°	C_D = 0.0001
F_N	Normal force	0.0008 $F_{N_{des}}$	C_D = 0.0001
F_C	Chord force	0.0008 $F_{C_{des}}$	C_D = 0.0001

The capacilities of pressure and temperature transducers are better than the requirements presented above. In general, the ability to determine forces and angle of attack is deficient by a factor of 2 to 3. It is expected that advanced calibration techniques taking into account temperature effects, nonlinearity, and hysteresis characteristics, as well as a careful ordering of the test program, will be required to achieve a significant improvement in the ability to resolve forces and moments. Application of modern optical techniques to the measurement angle of attack offer the most promise for an improvement in data accuracy.

6. CONCLUDING REMARKS

In this work, a major assumption is that the instrumentation is being used either at the full-scale design condition or as near to the condition (in the case of the balance) as dynamic conditions will allow. Further, the effects owing to Reynolds number have been assumed to be represented by basic tunnel instrumentation and calibration accuracy. The effects of noise on Reynolds number have been ignored. The latter seems to be a high-risk assumption and should be addressed to the point of resolution. A comparison of the relative magnitudes of the various contributions highlights the well-known fact that balance and angle-of-attack uncertainty are the largest contributors to the total uncertainty. A 50% reduction in the uncertainty of these two measurements would significantly reduce the overall uncertainty. The issue of flow curvature is one that bears watching, as does Mach gradient. The effects of these latter two quantities can become quite significant at cruise conditions with only very small increases.

In this paper, the analysis and comments are oriented toward static stability testing of a transport configuration. Other tests may show considerably different effects, and the user should examine his own test requirements and the consequences of uncertainties of the kind presented in this paper.

7. RECOMMENDATIONS

1. Strive to develop force and angle-of-attack instrumentation with one half the uncertainty of state-of-the-art instrumentation. This may require a rather exhaustive test technique to minimize hysteresis effects.

2. Research the role of aero-noise on Reynolds number effects.

3. Develop a standard calibration set of measurements and data reduction method for calibrating wind tunnels for flow quality. Obtain reference measurements in flight where applicable. A working group should be organized with the task of specifying the conditions and designing the calibration experiment.

4. Recommendation for future activities of the Conveners Group: Continue the activities of the group for at least another 2 years. As mentioned in the Introduction, there was not enough time to do a very thorough job. With the present base given, this should improve in the future, especially with regard to measurements other than force and moment measurements.

APPENDIX

CONVENERS GROUP

Eastern Atlantic Group

The first Eastern Atlantic meeting was held at the Hochschule der Bundeswehr München, Neubiberg, Germany, on May 8-9, 1980. The following were members and contributors.

P. Ashill, RAE, England
E. Barbantini, Aeritalia, Italy
P. Bradshaw, Imperial Col., England
A. Elsenaar, NLR, Netherlands
E. Erlich, ONERA, France
Ewald, VFW, Germany
H. P. Franz, VFW, Germany
Goldsmith, RAE, England
K. Kienappel, DFVLR, Germany
D. G. Mabey, RAE, England
K. C. Pallister, ARA, England
P. G. Pianta, Politecnico Torino, Italy
E. Stanewsky, DFVLR, Germany (convener)
E. Thiel, Dornier, Germany

Western Atlantic Group

The Western Atlantic Group met at NASA Ames Research Center, Moffett Field, California on October 28-29, 1980 and April 20-21, 1981. The following members participated in the preparation of this report:

Ronald Bengelink	Boeing, Seattle, Washington
Gerald Bowes	Boeing, Seattle, Washington
Denis Brown	NAE, Ottawa, Canada
Robert Buffington	Sandia Corp., Albuquerque, New Mexico
Joseph Cadwell	McDonnell Douglas, Long Beach, California
Milton Cohen	Rockwell International (NAAD), Los Angeles, California
Richard Frey	McDonnell Douglas, St. Louis, Missouri
Stanley Gottlieb	David Taylor Naval Ship Research and Development Center, Bethesda, Maryland

James Grunnet	Flui-Dyne, Minneapolis, Minnesota
W. D. Harvey	NASA Langley Research Center, Hampton, Virginia
E. Dabney Howe	Northrop Aircraft Corp., Hawthorne, California
F. Jackson	Calspan Corp., Tullahoma, Tennessee
John McAfee	Grumman Aerospace Corp., Bethpage, New York
A. Madsen	General Dynamics, Fort Worth, Texas
Frank Steinle (Convener)	NASA Ames Research Center, Moffett Field, California

The group also wishes to acknowledge the assistance of the following in providing valuable commentary during the preparation and revision of this report.

Roy Eaves	ARO, Inc. (now of Calspan Corp.), Tullahoma, Tennessee
David Benepe	General Dynamics, Fort Worth, Texas
Dr. Werner Pfenninger	NASA Langley Research Center, Hampton, Virginia

REFERENCES

1. Barche, J.: Experimental Data Base for Computer Program Assessment. Report of the Fluid Dynamic Panel Working Group 04, AGARD-AR-138, May 1979.

2. Reed, T. D.; Pope, T. C.; and Cooksey, J. M.: Calibration of Transonic and Supersonic Wind Tunnels. NASA CR-2920, 1977.

3. Winter, K. G.; and Smith, J. H. B.: A Comment on the Origin of End-Wall Interference in Wind-Tunnel Tests of Airfoils. RAE TM Aero 1816.

4. Barnwell, R. W.: A Similarity Rule for Compressibility and Side Wall Boundary Layer Effects in Two-Dimensional Wind Tunnels. AIAA Paper 79-0108, 1979.

5. Muhlstein, L.: and Coe, C. F.: Integration Time Required to Extract Accurate Data from Transonic Wind-Tunnel Tests. J. Aircraft, Vol. 16, No. 9, Sept. 1979, pp. 620-625.

6. Benek, J. A.: Effects of Acoustic and Vortical Disturbances on the Turbulent Boundary Layer at Freestream Mach Number 0.5. AEDC TR-77-73, 1977.

7. Weeks, D. J.; and Hodges, J.: An Experimental Investigation of the Influence of Acoustic Disturbances on the Development of a Turbulent Boundary Layer. ARC R & M 3825, 1978.

8. Meier, H. U.; and Kreplin, H.-P.: Influence of Freestream Turbulence on Boundary Layer Development. AIAA J., Vol. 18, No. 1, Jan. 1980, pp. 11-15.

9. Hartzuiker, J. P.; Pugh, P. G.; Lorenz-Meyer, W.; and Fasso, G. E.: On the Flow Quality Necessary for the Large European High-Reynolds-Number Transonic Wind Tunnel LEHRT. AGARD Report No. 644, Mar. 1976.

10. Mabey, D. G.: Flow Unsteadiness and Model Vibration in Wind Tunnels at Subsonic and Transonic Speeds. ARC CP No. 1155, 1971.

11. Brown, Clinton E.; and Chen, Chuan F.: An Analysis of Performance Estimation Methods for Aircraft. NASA CR-921, 1967.

12. MacWilkinson, D. G.; Blackerby, W. T.; and Paterson, J. H.: Correlation of Full-Scale Drag Predictions with Flight Measurements on the C-141A Aircraft, Phase II, Wind Tunnel Test, Analysis and Prediction Techniques. Vol. 1, Drag Predictions, Wind Tunnel Data Analysis and Correlation, NASA CR-2333, 1974.

13. Treon, S. L.; Steinle, F. W.; Hagerman, J. R.; Black, J. A.; and Buffington, R. J.: Further Correlation of Data from Investigations of a High-Subsonic-Speed Transport Aircraft Model in Three Major Transonic Wind Tunnels. AIAA Paper 71-291, Albuquerque, N.M., 1971.

14. Benek, J. A.; and High, M. D.: A Method for the Prediciton of the Effects of Free-Stream Disturbances on Boundary-Layer Transition. AEDC-TR-73-158, Oct. 1973.

15. Whitfield, J. D.; and Dougherty, N. S., Jr.: A Survey of Transition Research at AEDC. AGARD Fluid Dynamics Panel Symposium on Laminar-Turbulent Transition, Copenhagen, Denmark, May 2-4, 1977.

16. Reed, T. D.; Abu-Mostafa, A.; and Steinle, F. W.: Correlation of Preston-Tube Data with Laminar Skin Friction. AIAA Paper 82-0591, Williamsburg, Va., 1982.

17. Reed, T. D.; et al.: University Grant NSG-2396; Report pending, F. W. Steinle, Technical Monitor.

17a. Dougherty, N. S., Jr.; and Fisher, D. F.: Boundary Layer Transition on a 10-Degree Cone: Wind Tunnel/Flight Data Correlation. AIAA Paper 80-0154, Pasadena, Calif., 1980.

17b. Dougherty, N. S., Jr.; and Steinle, F. W., Jr.: Transition Reynolds Number Comparisons in Several Major Transonic Tunnels. AIAA Paper 74-627, Bethesda, Md., 1974.

17c. Mabey, D. G.: Boundary Layer Transition Measurements on the AEDC 10° Cone in Three RAE Wind Tunnels and Their Implications. Reports and Memoranda No. 3821, June 1976.

18. Isaacs, D.: Calibration of the RAE Bedford 8- by 8-Foot Wind Tunnel at Subsonic Speeds, Including a Discussion of the Corrections Applied to the Measured Pressure Distribution to Allow for the Direct and Blockage Effects Due to the Calibration Probe Shape. ARC R&M 3583, 1969.

19. Morris, D. E.; and Winter, K. G.: Requirements for Uniformity of Flow in Supersonic Wind Tunnels. RAE Tech Note AERO 2340, 1954.

20. Paterson, J. H.; Blackerby, W. T.; Schwanebeck, J. C.; and Braddock, W. F.: An Analysis of Flight Test Data on the C-141A Aircraft. NASA CR-1558, 1970.

21. Steinle, F. W., Jr.; and Pejack, E. R.: Toward an Improved Transonic Wind-Tunnel-Wall Geometry: A Numerical Study. AIAA Paper 80-0442, Colorado Springs, Colo., 1980.

22. Daugherty, J. C.: Wind Tunnel/Flight Correlation Study of Aerodynamic Characteristics of a Large Flexible Supersonic Cruise Airplane (XB-70-1). NASA TP-1514, 1979.

23. Wind Tunnel Design and Testing Techniques. Paper 26, AGARD CP-174, London, 6-8 Oct. 1975.

24. Holdhusen, J. S.: A Model Testing Technique for Determining Inlet Spillage Drag. 16th AIAA Turbine Engine Testing Working Group on Subscale Test and Simulation, May, 1976.

25. Bacon, J. W.; Pfenninger, W.; and Moore, C. R.: Investigation of a 30-Degree Swept and a 17-Foot Chord Straight Suction Wing in the Presence of Internal Sound, External Sounds, and Mechanical Vibrations, Summary of Laminar Boundary Layer Control Research. Vol. 1, ASD-TDR-65-554, 1964.

26. Carlson, J. C.; and Bacon, J. W.: Influence of Acoustical Disturbances in the Suction Ducting System on the Laminar Flow Control Characteristics of a 33° Swept Suction Wing. Northrop Report NOR-65-232, 1965.

27. El-Hady, N. M.: On the Stability of Three-Dimensional, Compressible Non-Parallel Boundary Layers. AIAA Paper 80-1374, 1980.

28. Bobitt, P. J.: Modern Fluid Dynamics of Subsonic and Transonic Flight, AIAA Paper 80-9861, 1980.

29. Pfenninger, W.; Reed, H. C.; and Dagenhart, T. R.: Design Considerations of Advanced Supercritical Low Drag Suction Airfoils. Symposium on Viscous Drag Reduction, Dallas, Tex., Nov. 7-8, 1979.

30. Harvey, William D.; Stainback, P. C.; and Owen, F. K.: Evaluation of Flow Quality in Two Large NASA Wind Tunnels at Transonic Speeds. NASA TP-1737, 1980.

31. Rose, W. C.; and Otten, L. J., III: Airborne Measurement of Atmospheric Turbulence. Proceedings of the Aero-Optics Symposium on Electromagnetic Wave Propagation from Aircraft, Apr. 1980 (NASA CP-2121).

32. Rose, W. C.; Craig, J.; and Raman, K. R.: Near-Field Aerodynamics and Optical Propagation Characteristics of a Large-Scale Turret Model. AFWL-TR-162, May 1981.

33. AGARDograph No. 186, Mar. 1974.

Table 1. Type of measurements and influence parameters

INFLUENCE-PARAMETERS / TYPE OF MEASUREMENTS	ACCURACY			FLOW NON-UNIFORMITY			FLOW UNSTEADYNESS			PURITY OF FLUID	CORRECT. FOR WIND TUNNEL WALL INTERFERENCE		SUPPORT INTERF. CORRECT.	MODEL DESIGN: (TOLER. + AEROEL.)	MEAS. OF + CORR. FOR AEROEL. EFFECTS (MODEL + SUPPORT)	
	PV	SC	CFD	TOTAL AND STATIC PRESS	VELOC./MACH N. / ANGULARITY	TEMP.	PRESS (ACOUST.)	VELOC. (VORTIC.)	TEMP. (SPOTS)		WALL INTERF.	SIDE-WALL EFFECTS			DEFORM.	VIBRAT.
TOTAL + STATIC PRESSURES												X				X
STEADY STATE: ΔCp	0.01	0.001	0.01	$\Delta Cp = 0.001$	$\Delta M = 0.001$ $\Delta\alpha = 0.1°$	O	O	O	O	O						
DYNAMIC: ΔCp						O		O	O	O						
BALANCE MEASUREMENTS				X	X	X	X	X	X	X	X		X	X	X	
LIFT C_L	0.01	0.001	0.01	77	77	77					77		77			
DRAG C_D	0.0005	0.0001	0.0001	$\Delta Pt = ½\%\ Pt$ $\Delta Cp = 0.001$	$\Delta M = 0.001$ $\Delta\alpha = 0.1°; 0.01°$	$\pm 1°$					$\Delta M = 0.001$ $\Delta\alpha = 0.01$		$\Delta Cp < 0.001$ $\Delta\alpha < 0.1°$ $\Delta\alpha < 0.01°$ * } +			
MOMENTS C_M	0.002	0.001	0.002	77	77	77					77					
COMPONENT FORCES																
PRESSURE DRAG																
BOUNDARY LAYERS				X	X	X	X	X	X	X			X	X		
MEAN QUANT.				$\Delta Pt = 0.2\%\ Pt$ $\Delta P = 0.2\%\ P$	SIMILAR TO	O	2% 9	0.1% U	0.5 K		O	O		$u_\tau\ k/\nu$		
FLUCT. QUANT.				77	BALANCE MEAS.	O					O	O		77		
HEAT TRANSFER				77		0.1 K					O	O		77		
UNSTEADY PHENOMENA				X	X	X	X	X						X	X	
BUFFETING				O	77	O	$\tilde{p}/q \simeq 0.5\%$									
FLUTTER				O	$\Delta M = 0.01$	± 2 K	$\sqrt{nF(n)} \cong 0.002$	O	O							
DYN. STAB.				O	77	O										
SIMUL. ENGINE FLOW				X $\Delta Cp = 0.005$	X $\Delta M = 0.001$	O	X $\tilde{P}_t/P_t < 0.01$	O	O	O			X		X	
REFLECTION PANE		X	X													

NOTES: PV = PERFORMANCE VERIFICATION; SC = SMALL CONFIGURATIONAL CHANGES; CFD = COMPUTATIONAL FLUID DYNAMICS; O = NOT CONSIDERED CRITICAL; BLANK = NOT CONSIDERED EXPLICITLY; X = DISCUSSED WITHIN TEXT; + = TAIL; * = WING.

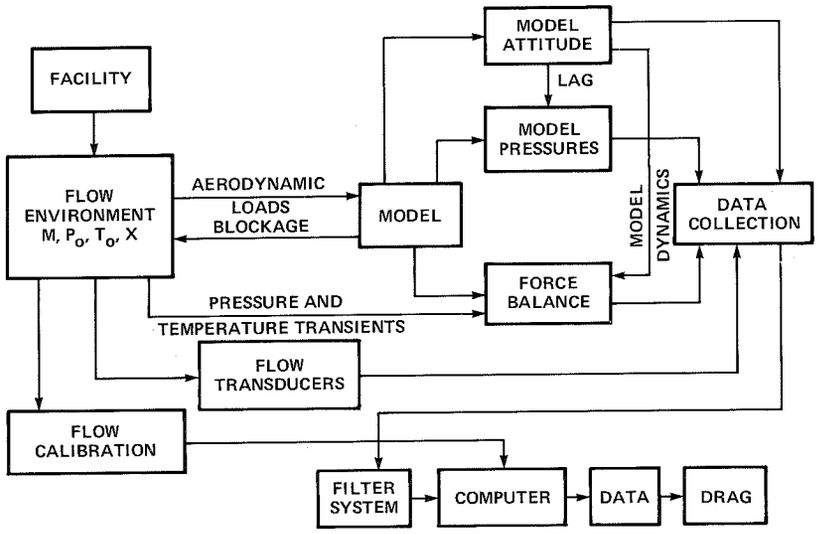

Figure 1. Data and error flow diagram.

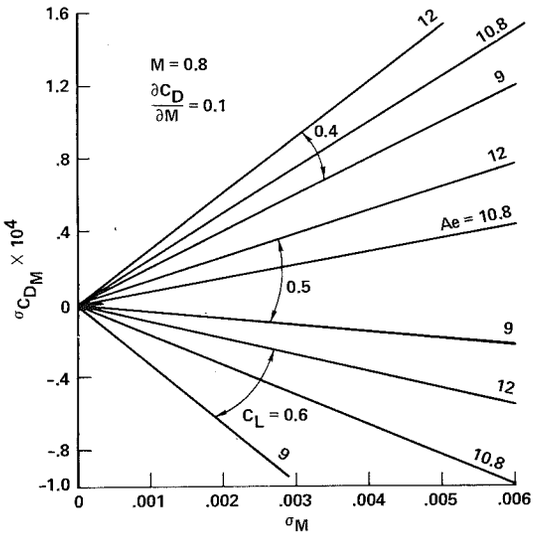

Figure 2. Effect of σ_M on σ_{C_D}.

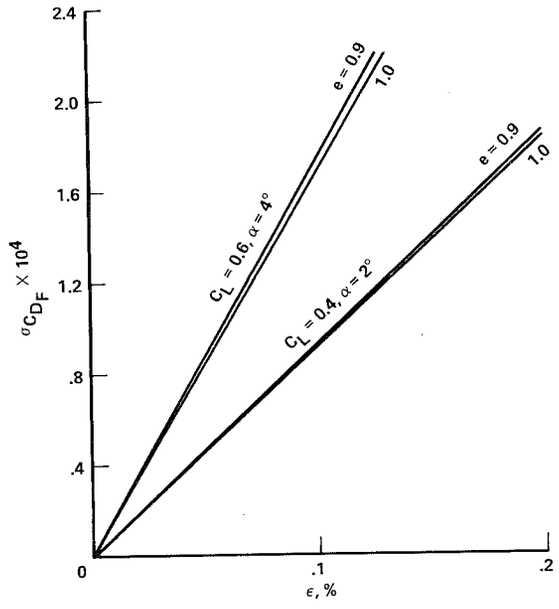

Figure 3. Deviation in C_D due to normal-force and chord-force deviation.

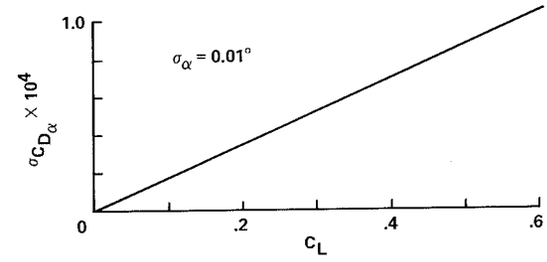

Figure 4. Effect of deviation in angle of attack on C_D.

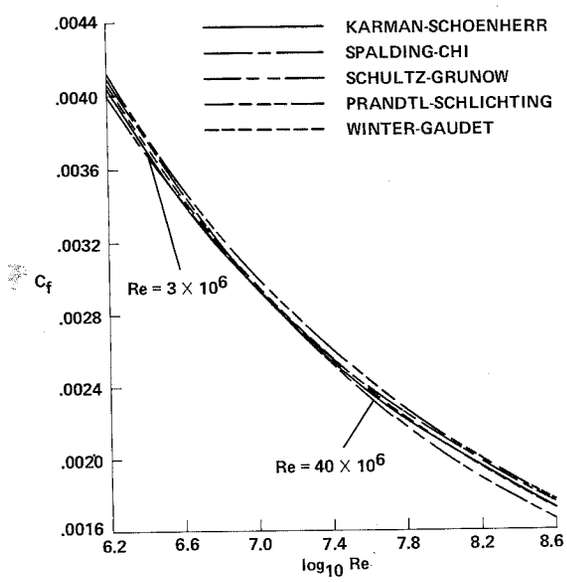

Figure 5. Comparison of empirical flat-plate skin-friction formulae for incompressible turbulent flow.

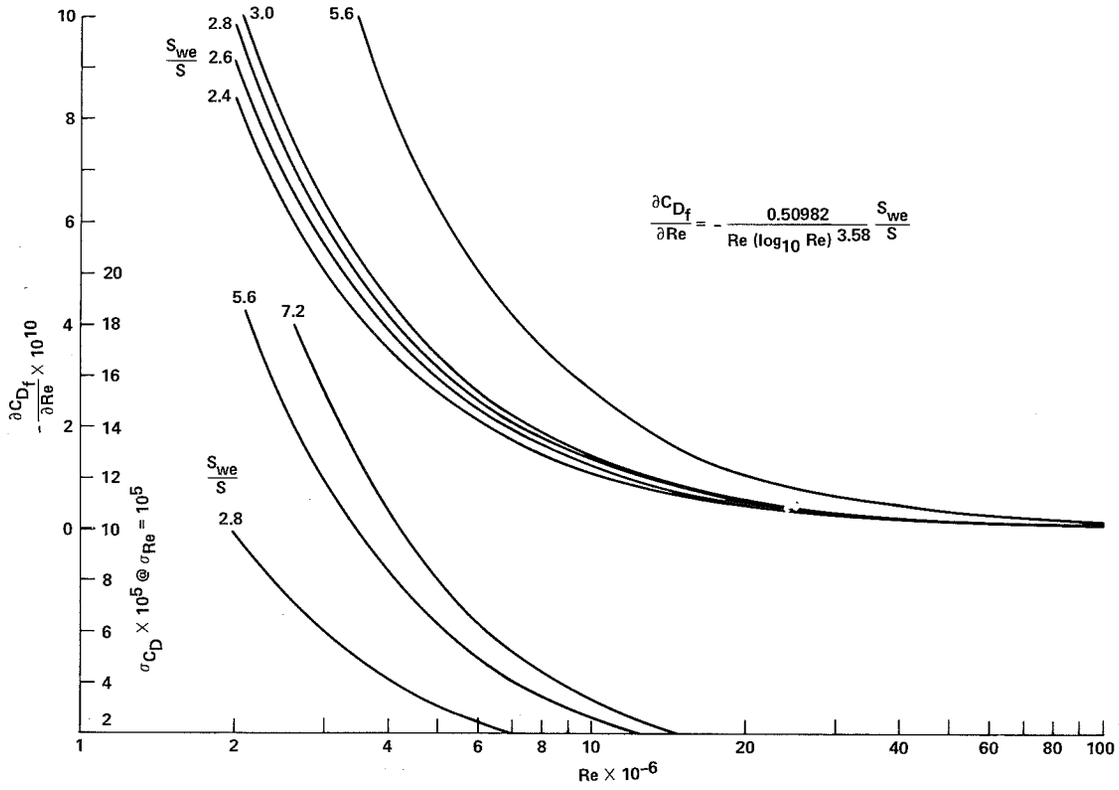

Figure 6. Effect of Reynolds number deviation on C_D.

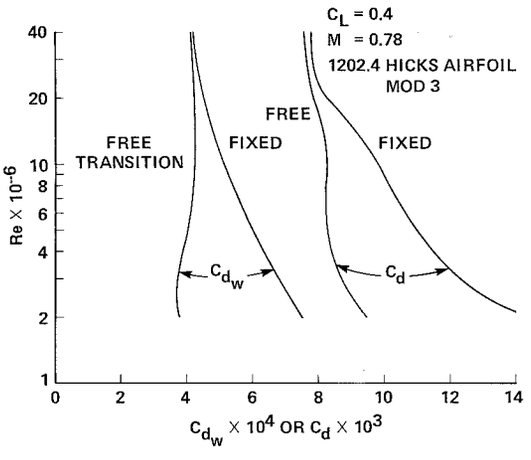

Figure 7. Comparison of transition effects, modified 1202.4 airfoil.

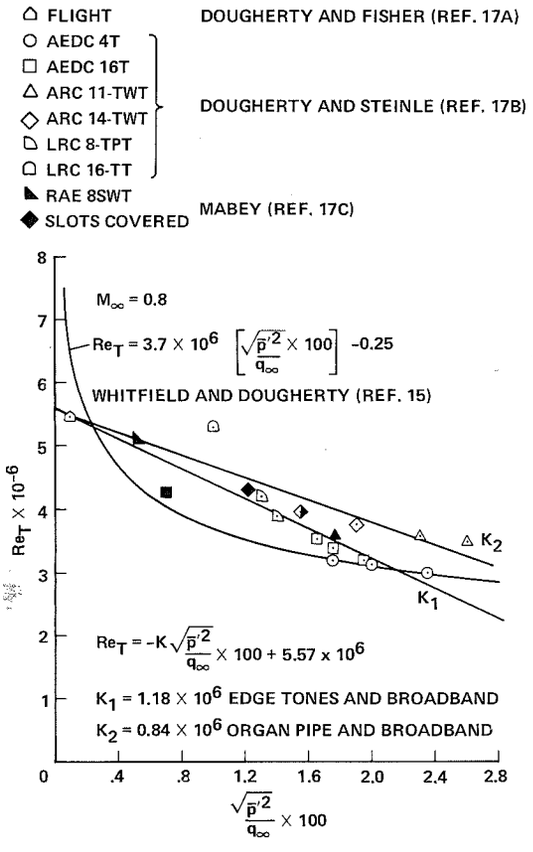

Figure 8. Effect of noise on boundary-layer transition.

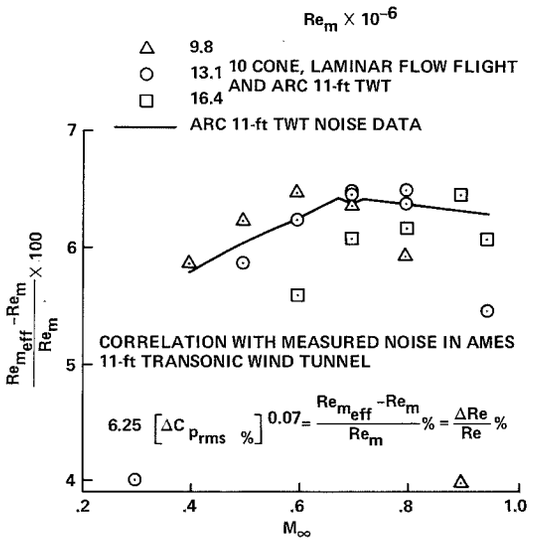

Figure 9. Estimate of effective Reynolds number based on analysis of flight data.

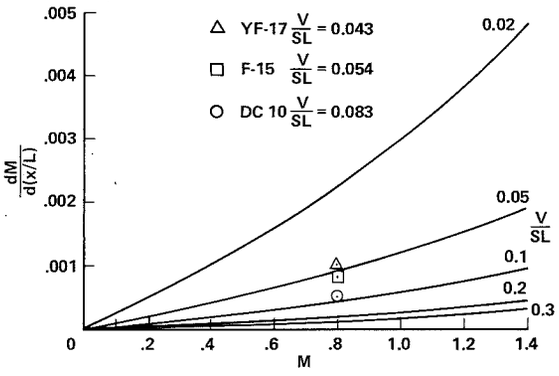

Figure 10. Mach number gradient per model length for $\sigma_{C_{D_{[dM/(dx/L)]}}} = 0.0001$.

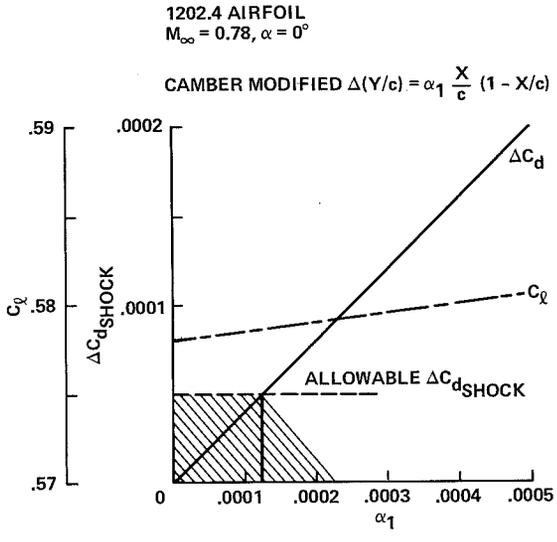

Figure 11. Effect of induced camber on section lift and shock drag, 1202.4 airfoil.

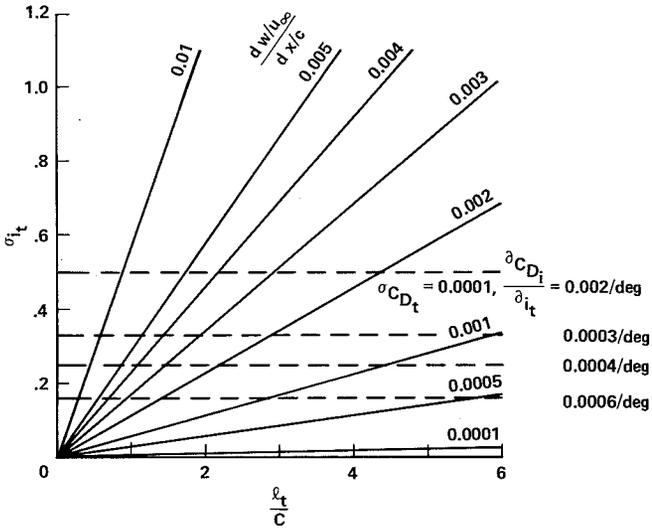

Figure 12. Contribution of flow curvature to $\sigma_{C_{D_t}}$.

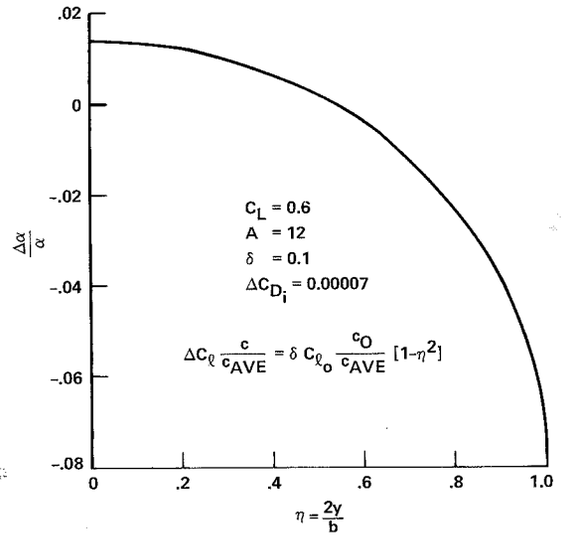

Figure 13. Effect of adding parabolic lift distribution to elliptically loaded wing.

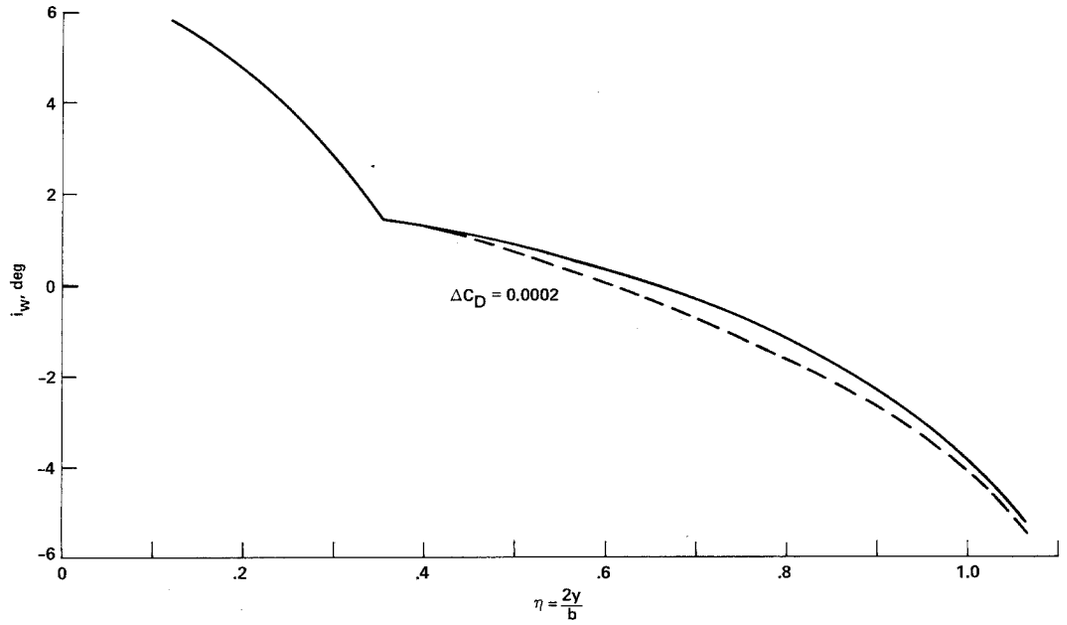

Figure 14. Effect of spanwise variation of twist on drag for a modern transport-type wing.

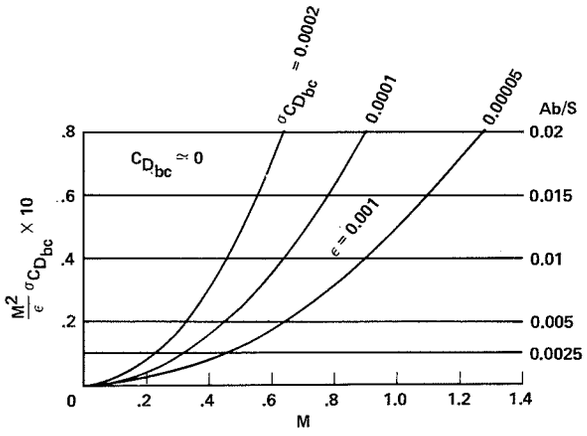

Figure 15. Contribution of pressure deviation to base or cavity drag.

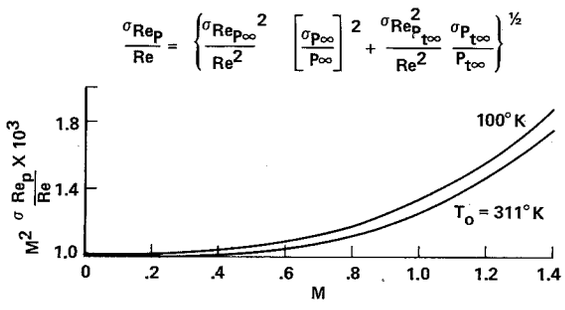

Figure 17. Deviation in Re because of static and total pressure deviation.

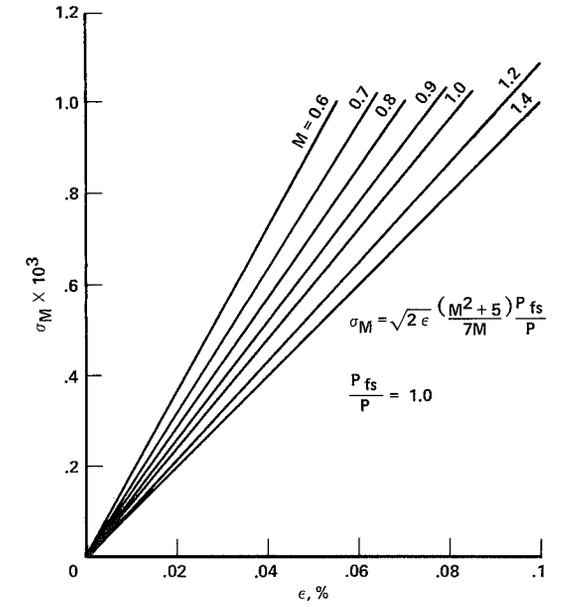

Figure 16. Deviation in M because of pressure transducer deviation.

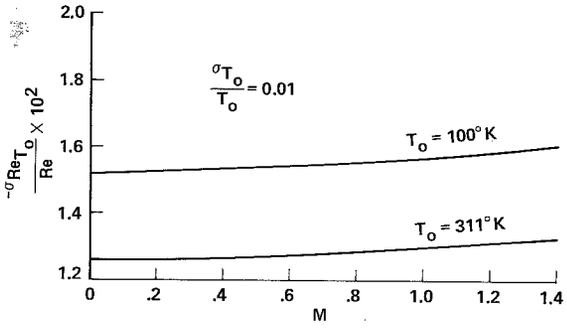

Figure 18. Effect of σ_{T_o} on $\sigma_{Re_{T_o}}$.

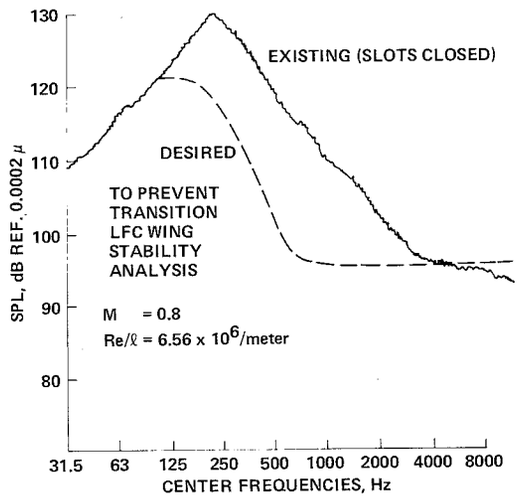

Figure 19. Sound pressure level versus frequency.

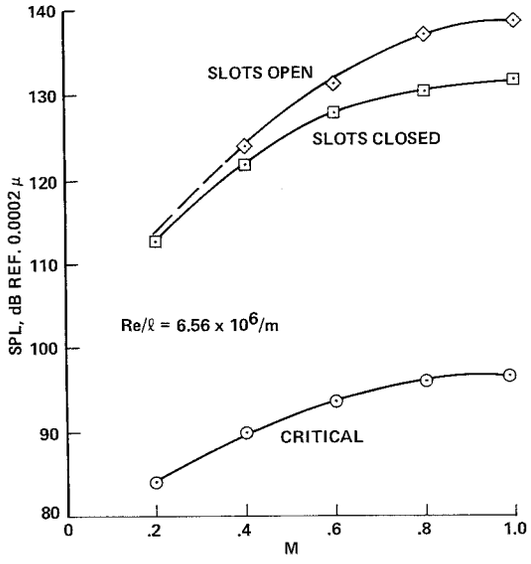

Figure 21. Effect of M on critical SPL for LFC testing.

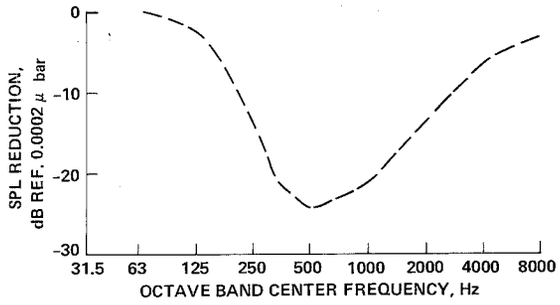

Figure 20. Required reduction in dB to prevent transition.

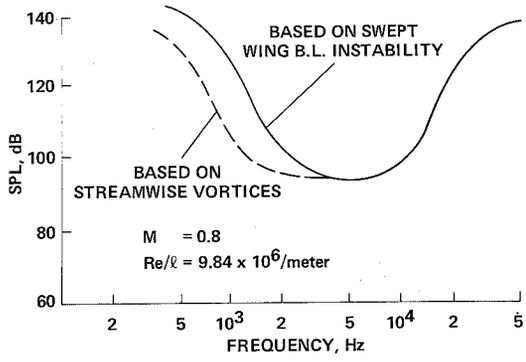

Figure 22. Critical disturbance level versus frequency for LFC testing.

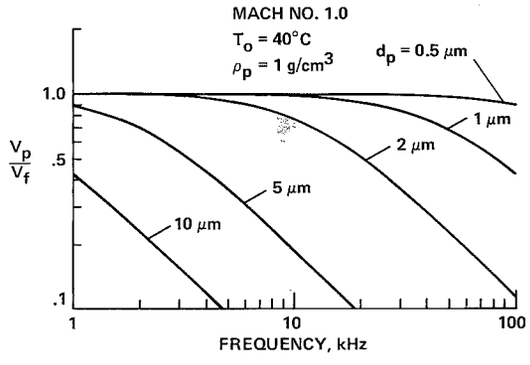

Figure 23. Effect of particle diameter on frequency response.

REPORT DOCUMENTATION PAGE

1. Recipient's Reference	2. Originator's Reference	3. Further Reference	4. Security Classification of Document
	AGARD-AR-184	ISBN 92-835-1440-8	UNCLASSIFIED

5. Originator Advisory Group for Aerospace Research and Development
North Atlantic Treaty Organization
7 rue Ancelle, 92200 Neuilly sur Seine, France

6. Title

WIND TUNNEL FLOW QUALITY AND DATA ACCURACY REQUIREMENTS

7. Presented at

8. Author(s)/Editor(s)	9. Date
See Flyleaf	November 1982
10. Author's/Editor's Address	**11. Pages**
See Flyleaf	30

12. Distribution Statement This document is distributed in accordance with AGARD policies and regulations, which are outlined on the Outside Back Covers of all AGARD publications.

13. Keywords/Descriptors

Wind tunnels	Experimental data
Fluid flow	Data acquisition
Quality	Accuracy

14. Abstract

This Advisory Report includes the results of three meetings sponsored by the Windtunnel Testing Techniques Sub-Committee of the Fluid Dynamics Panel among experts in the subject area. Conclusions and recommendations for future work were drawn by the meeting chairmen. This report is a companion to AGARD Advisory Report AR-174 on "Windtunnel Capability Related to Test Sections, Cryogenics, and Computer-Windtunnel Integration" published April 1982, which reports the results of similar meetings convened on those topics.

This Advisory Report was prepared for the Fluid Dynamics Panel of AGARD.

AGARD Advisory Report No.184 Advisory Group for Aerospace Research and Development, NATO WIND TUNNEL FLOW QUALITY AND DATA ACCURACY REQUIREMENTS by F.Steinle and E.Stanewsky Edited by R.O.Dietz Published November 1982 30 pages This Advisory Report includes the results of three meetings sponsored by the Windtunnel Testing Techniques Sub-Committee of the Fluid Dynamics Panel among experts in the subject area. Conclusions and recommendations for future work were drawn by the meeting chairmen. This report is a companion to AGARD P.T.O.	AGARD-AR-184 Wind tunnels Fluid flow Quality Experimental data Data acquisition Accuracy	AGARD Advisory Report No.184 Advisory Group for Aerospace Research and Development, NATO WIND TUNNEL FLOW QUALITY AND DATA ACCURACY REQUIREMENTS by F.Steinle and E.Stanewsky Edited by R.O.Dietz Published November 1982 30 pages This Advisory Report includes the results of three meetings sponsored by the Windtunnel Testing Techniques Sub-Committee of the Fluid Dynamics Panel among experts in the subject area. Conclusions and recommendations for future work were drawn by the meeting chairmen. This report is a companion to AGARD P.T.O.	AGARD-AR-184 Wind tunnels Fluid flow Quality Experimental data Data acquisition Accuracy
AGARD Advisory Report No.184 Advisory Group for Aerospace Research and Development, NATO WIND TUNNEL FLOW QUALITY AND DATA ACCURACY REQUIREMENTS by F.Steinle and E.Stanewsky Edited by R.O.Dietz Published November 1982 30 pages This Advisory Report includes the results of three meetings sponsored by the Windtunnel Testing Techniques Sub-Committee of the Fluid Dynamics Panel among experts in the subject area. Conclusions and recommendations for future work were drawn by the meeting chairmen. This report is a companion to AGARD P.T.O.	AGARD-AR-184 Wind tunnels Fluid flow Quality Experimental data Data acquisition Accuracy	AGARD Advisory Report No.184 Advisory Group for Aerospace Research and Development, NATO WIND TUNNEL FLOW QUALITY AND DATA ACCURACY REQUIREMENTS by F.Steinle and E.Stanewsky Edited by R.O.Dietz Published November 1982 30 pages This Advisory Report includes the results of three meetings sponsored by the Windtunnel Testing Techniques Sub-Committee of the Fluid Dynamics Panel among experts in the subject area. Conclusions and recommendations for future work were drawn by the meeting chairmen. This report is a companion to AGARD P.T.O.	AGARD-AR-184 Wind tunnels Fluid flow Quality Experimental data Data acquisition Accuracy

Advisory Report AR-174 on "Windtunnel Capability Related to Test Sections, Cryogenics, and Computer-Windtunnel Integration" published April 1982, which reports the results of similar meetings convened on those topics.

This Advisory Report was prepared for the Fluid Dynamics Panel of AGARD.

ISBN 92-835-1440-8

Advisory Report AR-174 on "Windtunnel Capability Related to Test Sections, Cryogenics, and Computer-Windtunnel Integration" published April 1982, which reports the results of similar meetings convened on those topics.

This Advisory Report was prepared for the Fluid Dynamics Panel of AGARD.

ISBN 92-835-1440-8

Advisory Report AR-174 on "Windtunnel Capability Related to Test Sections, Cryogenics, and Computer-Windtunnel Integration" published April 1982, which reports the results of similar meetings convened on those topics.

This Advisory Report was prepared for the Fluid Dynamics Panel of AGARD.

ISBN 92-835-1440-8

Advisory Report AR-174 on "Windtunnel Capability Related to Test Sections, Cryogenics, and Computer-Windtunnel Integration" published April 1982, which reports the results of similar meetings convened on those topics.

This Advisory Report was prepared for the Fluid Dynamics Panel of AGARD.

ISBN 92-835-1440-8

AGARD
NATO OTAN
7 RUE ANCELLE · 92200 NEUILLY-SUR-SEINE
FRANCE
Telephone 745.08.10 · Telex 610176

DISTRIBUTION OF UNCLASSIFIED AGARD PUBLICATIONS

AGARD does NOT hold stocks of AGARD publications at the above address for general distribution. Initial distribution of AGARD publications is made to AGARD Member Nations through the following National Distribution Centres. Further copies are sometimes available from these Centres, but if not may be purchased in Microfiche or Photocopy form from the Purchase Agencies listed below.

NATIONAL DISTRIBUTION CENTRES

BELGIUM
Coordonnateur AGARD – VSL
Etat-Major de la Force Aérienne
Quartier Reine Elisabeth
Rue d'Evere, 1140 Bruxelles

CANADA
Defence Science Information Services
Department of National Defence
Ottawa, Ontario K1A OK2

DENMARK
Danish Defence Research Board
Østerbrogades Kaserne
Copenhagen Ø

FRANCE
O.N.E.R.A. (Direction)
29 Avenue de la Division Leclerc
92320 Châtillon sous Bagneux

GERMANY
Fachinformationszentrum Energie,
Physik, Mathematik GmbH
Kernforschungszentrum
D-7514 Eggenstein-Leopoldshafen 2

GREECE
Hellenic Air Force General Staff
Research and Development Directorate
Holargos, Athens

ICELAND
Director of Aviation
c/o Flugrad
Reykjavik

ITALY
Aeronautica Militare
Ufficio del Delegato Nazionale all'AGARD
3, Piazzale Adenauer
Roma/EUR

LUXEMBOURG
See Belgium

NETHERLANDS
Netherlands Delegation to AGARD
National Aerospace Laboratory, NLR
P.O. Box 126
2600 A.C. Delft

NORWAY
Norwegian Defence Research Establishment
Main Library
P.O. Box 25
N-2007 Kjeller

PORTUGAL
Direcção do Serviço de Material
da Forca Aerea
Rua da Escola Politécnica 42
Lisboa
Attn: AGARD National Delegate

TURKEY
Department of Research and Development (ARGE)
Ministry of National Defence, Ankara

UNITED KINGDOM
Defence Research Information Centre
Station Square House
St. Mary Cray
Orpington, Kent BR5 3RE

UNITED STATES
National Aeronautics and Space Administration (NASA)
Langley Field, Virginia 23365
Attn: Report Distribution and Storage Unit

THE UNITED STATES NATIONAL DISTRIBUTION CENTRE (NASA) DOES NOT HOLD STOCKS OF AGARD PUBLICATIONS, AND APPLICATIONS FOR COPIES SHOULD BE MADE DIRECT TO THE NATIONAL TECHNICAL INFORMATION SERVICE (NTIS) AT THE ADDRESS BELOW.

PURCHASE AGENCIES

Microfiche or Photocopy

National Technical
Information Service (NTIS)
5285 Port Royal Road
Springfield
Virginia 22161, USA

Microfiche

Space Documentation Service
European Space Agency
10, rue Mario Nikis
75015 Paris, France

Microfiche or Photocopy

British Library Lending
Division
Boston Spa, Wetherby
West Yorkshire LS23 7BQ
England

Requests for microfiche or photocopies of AGARD documents should include the AGARD serial number, title, author or editor, and publication date. Requests to NTIS should include the NASA accession report number. Full bibliographical references and abstracts of AGARD publications are given in the following journals:

Scientific and Technical Aerospace Reports (STAR)
published by NASA Scientific and Technical
Information Facility
Post Office Box 8757
Baltimore/Washington International Airport
Maryland 21240, USA

Government Reports Announcements (GRA)
published by the National Technical
Information Services, Springfield
Virginia 22161, USA

Printed by Technical Editing and Reproduction Ltd
5–11 Mortimer Street, London W1N 7RH

ISBN 92-835-1440-8